Journal of Banking & Finance 59 (2015) 202–219

Contents lists available at ScienceDirect

Journal of Banking & Finance

journal homepage: www.elsevier.com/locate/jbf

Liquidity-adjusted Intraday Value at Risk modeling and risk management: An application to data from Deutsche Börse ☆

Georges Dionne [a,b,*], Maria Pacurar [c], Xiaozhou Zhou [b,d]

[a] Canada Research Chair in Risk Management, HEC Montréal, Montréal H3T 2A7, Canada
[b] Finance Department, HEC Montréal, Montréal H3T 2A7, Canada
[c] Rowe School of Business, Dalhousie University, Halifax B3H 4R2, Canada
[d] Faculty of Management (ESG), University of Quebec at Montreal (UQAM), H3C 3P8, Canada

ARTICLE INFO

Article history:
Received 10 November 2014
Accepted 11 June 2015
Available online 24 June 2015

JEL classification:
C22
C41
C53
G11

Keywords:
Liquidity-adjusted Intraday Value at Risk
Tick-by-tick data
Log-ACD-VARMA-MGARCH
Ex-ante liquidity premium
Limit Order Book

ABSTRACT

This paper develops a high-frequency risk measure: the Liquidity-adjusted Intraday Value at Risk (LIVaR). Our objective is to explicitly consider the endogenous liquidity dimension associated with order size. By reconstructing the open Limit Order Book of Deutsche Börse, changes in the tick-by-tick (ex-ante) frictionless return and actual return are modeled jointly. The risk related to the ex-ante liquidity premium is then quantified. Our model can be used to identify the impact of ex-ante liquidity risk on total risk, and to provide an estimation of the VaR for the actual return at a point in time. In our sample, liquidity risk can account for up to 32% of total risk depending on order size.

1. Introduction

Following increased computerization, many prominent exchanges around the world such as Euronext, the Tokyo Stock Exchange, the Toronto Stock Exchange and the Australian Stock Exchange have organized trading activities under a purely automatic order-driven structure: there are no designated market-makers during continuous trading, and liquidity is fully guaranteed by market participants via an open Limit Order Book (LOB hereafter). In other main exchange markets including the NYSE and the Frankfurt Stock Exchange, trading activities are carried out under the hybrid structure, which combines the automatic order-driven structure and the traditional floor-based quote-driven structure. Nevertheless, most trades are executed under the automatic order-driven structure due to its advantages of transparency, efficiency and immediacy. Consequently, trading frequency is rising and trading activity is easier than ever.

As mentioned above, one of the most important features of open LOB is that liquidity is provided entirely by traders who place limit orders. As a result, the role of the traditional market makers has been replaced by informed and uninformed traders.[1] During trading hours, traders can place limit orders with different prices

☆ We thank Yann Bilodeau for his help in constructing the dataset and comments. We also thank Diego Amaya, Tolga Cenesizoglu, Bidisha Chakrabarty, Christian Gourieroux, Philippe Gregoire, Elisa Luciano, Mohamed Mekhaimer, Benoit Perron, Ruilin Tian, Gabriel Yergeau and participants at the 53rd Annual meeting of the Société canadienne de science économique, 2013 Canadian Economics Association Conference, 2014 Midwest Finance Association Annual Meeting, 7th Financial Risks International Forum, 2014 Northern Finance Association Annual Meeting and 2014 Financial Management Association Annual Meeting for their remarks. Georges Dionne and Maria Pacurar acknowledge financial support from the Social Sciences and Humanities Research Council (SSHRC) in Canada (#435-2012-1503 and #410-2009-0229, respectively), and Xiaozhou Zhou thanks the Fonds de Recherche sur la société et la culture du Québec (FRQSC) and the Centre Interuniversitaire sur le Risque, les Politiques Economiques et l'Emploi (CIRPEE) for financial support. The authors also acknowledge financial support from the Canadian Foundation for Innovation for the acquisition of data and computer facilities. They are thankful to two anonymous referees for their helpful comments.

* Corresponding author at: Canada Research Chair in Risk Management, HEC Montréal, Montréal H3T 2A7, Canada. Tel.: +1 514 340 6596.

E-mail addresses: georges.dionne@hec.ca (G. Dionne), maria.pacurar@dal.ca (M. Pacurar), xiao-zhou.zhou@hec.ca (X. Zhou).

[1] A large number of studies show that informed traders trade via open LOB (Kumar and Seppi, 1994; Handa and Schwartz, 1996; Bloomfield et al., 2005; Foucault et al., 2005; Kaniel and Liu, 2006; Rosu, 2009, among others).

http://dx.doi.org/10.1016/j.jbankfin.2015.06.005
0378-4266/

and quantities according to their trading strategies and preferences. Nowadays, these limit orders are placed, updated or canceled very frequently. As a result, the liquidity embedded in the open LOB also changes quickly. Another important feature of the open LOB market structure is the existence of active trading[2] whereby traders trade over a very short time horizon by monitoring the market continuously or using high-speed computers during the day and liquidating all open positions before market closing. Leaving aside the question of whether active trading is beneficial or not,[3] this new trading culture requires more and more attention to intraday risk derived from market and open LOB. However, traditional risk management has been challenged by this trend towards high-frequency trading because low-frequency measures of risk such as Value at Risk (VaR), which are usually based on daily data, are ill-suited to capturing the potential liquidity risk hidden in very short horizons.

In this paper, we propose a new high-frequency risk measure—Liquidity-adjusted Intraday Value at Risk (LIVaR)—that accounts for both the market risk and the ex-ante liquidity risk of liquidating a position.[4] Ex-ante liquidity is computed for a given order size before the transaction is executed. The difference between ex-ante liquidity and traditional (ex-post) liquidity is that the latter is the liquidity consumed when transactions are completed.[5] By its nature, ex-ante liquidity is forward-looking liquidity and presents important and practical aspects for intraday traders and other participants indirectly involved in active trading, including financial institutions[6] and market regulators. Most importantly, compared with the ex-post liquidity measure, the ex-ante liquidity measure is more related to the original definition of a liquid asset. Typically, the recognized description of a liquid security is its ability to convert the *desired quantity* of a financial asset into cash *quickly* and with little *impact on the market price* (Demsetz, 1968; Black, 1971; Kyle, 1985; Glosten and Harris, 1988). This definition implicitly covers four dimensions: *volume* (significant quantity), *price impact* (deviation from the best price provided in the market), *time* (speed of completing the transaction), and *resilience* (speed of backfilling). The ex-ante liquidity measure derived from open LOB can provide more information on volume, price impact and resilience dimensions. In an automated trading system, the speed of completing the transaction varies according to the location and the capacity of the machine and software.

Regarding existing risk measures, the conventional VaR is a risk measure that has been widely used in both academic and industry sectors. However, at both low frequency and high frequency, this risk measure can be interpreted only as an estimation of the potential loss on a predetermined portfolio over a relatively long or short fixed period, namely a measure of market price risk. Thus, VaR is not a liquidation value because it does not take into account the volume dimension; it is solely a 'paper value' for a frozen portfolio. Nevertheless, liquidity risk is always present before the transaction is realized. Further, from a high-frequency market microstructure perspective, the transaction price is an outcome of information shock, trading environment, market imperfections, and the state of the LOB. For very short horizons, all these microstructure effects could cause the transaction price to deviate from the efficient price. Therefore, if we concentrate on the transaction price, the VaR will suffer from a serious omission of liquidity, especially when the liquidation quantity is large. To unwind a large position, a trader might have to move down in the LOB and accept a lower price. In other words, when a trader with a large long position for a given stock wishes to liquidate his position in a very short time horizon, his potential loss will depend on two (related) risks: market risk and liquidity risk. Market risk is assumed by all traders, whereas liquidity risk is a concern only when the trader starts liquidating his position. This is why our proposed LIVaR measure includes the additional dimension of ex-ante liquidity risk. LIVaR measures the potential maximum loss at a given confidence level due to the decrease in both market price and available liquidity in the LOB. The introduction of the ex-ante liquidity dimension can thus offer a more accurate risk measure for active traders and market regulators who aim to closely monitor total risk and compute regulatory capital.

Very few studies have focused on high-frequency risk measures. Dionne et al. (2009) are the first to consider an ultra-high-frequency market risk measure, Intraday Value at Risk (IVaR), based on *all* transactions. In their study, the informative content of trading frequency is taken into account by modeling the durations between two consecutive transactions. One important practical contribution of their paper is that instead of being restricted to traditional one- or five-minute horizons, their model allows the IVaR measure to be computed for any time horizon once the model is estimated. The authors found that ignoring the effect of durations can underestimate risk. However, as they noted, similar to other VaR measures, the IVaR ignores the ex-ante liquidity dimension by taking into account only information about transaction prices.

The development of liquidity-adjusted risk measures goes back to Bangia et al. (1999), who first consider the spread between best ask and bid as a measure of liquidity risk in VaR computation. To simplify the modeling, they further assume that the liquidity risk proxied by half spread is perfectly correlated with market risk. Actually, the total risk they attempt to identify is the sum of market risk and trading cost associated with only one share, because their liquidity risk measure does not consider the volume dimension. In line with Bangia et al. (1999), Angelidis and Benos (2006) estimate the liquidity-adjusted VaR by using data from the Athens Stock Exchange. They find that liquidity risk measured by the bid-ask spread accounts for 3.4% of total market risk for high-capitalization stocks and 11% for low-capitalization stocks. Using the same framework as Bangia et al. (1999), Weiß and Supper (2013) address the liquidity risk of a portfolio formed with five NASDAQ stocks by estimating the multivariate distribution of log-return and spread using vine copulas to account for the dependence between the two variables across stocks over a regular interval of 5 min. They evidence strong extreme co-movements in liquidity and tail dependence between bid-ask spreads and log-returns across the selected stocks.

Our study is related to that of Giot and Grammig (2006), who focus on the ex-ante liquidity risk faced by an impatient trader acting as a liquidity demander by submitting a market order. Using open LOB Xetra data sampled at regular time intervals, the authors construct an actual return that is a potential implicit return for a predetermined volume to trade over a fixed time horizon of 10 or 30 min. Ex-ante liquidity risk is quantified by comparing the standard VaR based on frictionless return, i.e., mid-quote return, and the liquidity-adjusted VaR inferred from the actual return.

Our study differs from previous papers in the following ways. First, we examine the ex-ante liquidity risk by focusing on the tick-by-tick frictionless returns (issued from the best bid/ask price)

[2] High-frequency trading (HFT) was estimated to make up 51% of equity trades in the U.S. in 2012 and 39% of traded value in the European cash markets (Tabb Group). In this study, we distinguish between active traders and high-frequency traders. As mentioned in Aït-Sahalia and Saglam (2014), HFT refers to trading strategies whose profits strongly rely on a latency advantage. Our active traders include traders using algorithmic strategies and traders working manually at their trading desks.

[3] HFT was strongly criticized after the "flash crash" on May 6, 2010, and "gold halt" on January 6, 2014. However, HFT has been shown to increase market liquidity (Hendershott et al., 2011) and price efficiency (Chaboud et al., 2014; Brogaard et al., 2014).

[4] In this paper we consider the case of a sell transaction, but similar arguments apply to a buy transaction.

[5] The ex-post measure is based on the transaction price and is therefore backward-looking.

[6] As mentioned by Gouriéroux and Jasiak (2010), financial institutions also need intraday risk analysis for internal control of their trading desks.

and actual returns (issued from the potential liquidation price) derived from open LOB. Many papers have explored ex-post liquidity (Bacidore et al., 2003; Battalio et al., 2003; Goyenko et al., 2009, among others), which is already consumed by the market or marketable orders when the trades are realized. Compared with ex-post liquidity, ex-ante liquidity is more informative and relevant in that it measures the unconsumed liquidity in LOB. Further, the existing literature that analyzes ex-ante measures of liquidity (e.g., Giot and Grammig, 2006) is based on a regular time interval and thus ignores the information within the interval. In our study, we find that the durations between two consecutive observations are positively related to volatilities of actual returns and frictionless returns.

Second, our study addresses the questions of the relationship between ex-ante liquidity risk embedded in open LOB and market risk, and how ex-ante liquidity evolves during the trading day. One challenge of directly modeling frictionless returns and actual returns is that they are not time-additive. Therefore, we model the frictionless return changes and actual return changes using an econometric model characterized by the Logarithmic Autoregressive Conditional Duration, Vector Autoregressive Moving Average and Multivariate GARCH processes (denoted by Log-ACD, VARMA and M-GARCH hereafter). The structure not only captures the joint dynamics of both frictionless return changes and actual return changes, but also quantifies the impact of ex-ante liquidity risk on total risk by further defining $IVaR^c$ and $LIVaR^c$ as the VaRs on frictionless return changes and actual return changes, respectively. To make the model more flexible, we allow for the time-varying correlation of volatility of the frictionless return and actual return.

Third, from a practical perspective, our proposed risk measure aims at providing a view of total risk and ex-ante liquidity that can help high-frequency traders develop their timing strategies during a particular trading day. Our model is first estimated on deseasonalized data and then validated on both simulated deseasonalized and re-seasonalized data. The time series of re-seasonalized data is constructed by re-introducing deterministic seasonality factors. One advantage of simulated re-seasonalized data is that risk management can be conducted in calendar time. In addition, because the model is estimated using tick-by-tick observations and takes into account the durations between two consecutive transactions, practitioners can then construct the risk measure for any desired time horizon.[7]

The rest of the paper is organized as follows: Section 2 describes the dataset we utilize. Section 3 briefly presents the procedure used to test the model and to compute an impact coefficient of ex-ante liquidity risk and an ex-ante liquidity premium. Section 4 defines the actual return, frictionless return, IVaR and LIVaR. In Section 5, we specify the econometric model used to capture the dynamics of duration, frictionless return changes, actual return changes and their correlations. Section 6 applies the econometric model proposed in Section 5 to data for three stocks and reports the estimation results. The model performance is assessed by the unconditional coverage test of Kupiec (1995), the independence test proposed by Christoffersen (1998), and the new backtests of Ziggel et al. (2014). In Section 7, we analyze the ex-ante liquidity risk in $LIVaR^c$ and compare the proposed LIVaR with other high-frequency risk measures. Section 8 explores the robustness of our results by considering a different sample period and simulations with different volatilities for actual returns and extreme events. Section 9 concludes the paper and proposes new research directions.

2. Xetra dataset

The present study uses data from the automated order-driven trading system Xetra, which is operated by Deutsche Börse at the Frankfurt Stock Exchange and has a similar structure to NASDAQ's Integrated Single Book and NYSE's Super Dot. A more detailed review of Xetra can be found in Supplementary web-based Appendix. Our sample period is July 5 to July 16, 2010. For robustness, an additional sample from June 6 to June 17, 2011, is considered.

For blue-chip and other highly liquid stocks, during continuous trading, there are no dedicated market makers like the traditional NYSE specialists. Therefore, the liquidity comes from all market participants who submit limit orders in LOB. Our database includes up to 20 levels of LOB information except the hidden part of an iceberg order, which means that by observing the LOB, any trader and registered member can monitor the dynamic of liquidity supply and potential price impact caused by a market or marketable limit order. However, all the trading and order submissions are anonymous, that is, the state and the updates on LOB can be observed but there is no information on the identities of market participants.

The raw dataset that we analyzed contains all the events that are tracked and sent through the data streams. There are two main types of streams: delta and snapshot. The former tracks all the possible updates in LOB such as entry, revision, cancelation and expiration. Traders can be connected to the delta stream during trading hours to receive the latest information, whereas the snapshot provides an overview of the state of LOB and is sent after a constant time interval for a given stock. Xetra original data with delta and snapshot messages are first processed using the software Xetra Parser developed by Bilodeau (2013) to make Deutsche Börse Xetra raw data usable for academic and professional purposes. Xetra Parser reconstructs the real-time order book sequence including all the information for both auctions and continuous trading by implementing the Xetra trading protocol and Enhanced Broadcast.[8] We further convert the raw LOB information into a readable LOB for each update time and then retrieve useful and accurate information about the state of LOB and the precise timestamp for order modifications and transactions during continuous trading. Inter-trade durations and LOB update durations are irregular. The stocks that we choose for this study—SAP (SAP), RWE AG (RWE), and Merck (MRK)—are blue-chip stocks from the DAX30 index. SAP is a leading multinational software corporation with a market capitalization of 33.84 billion Euros in 2010. RWE generates and distributes electricity to various customers including municipal, industrial, commercial and residential customers. The company produces natural gas and oil, mines coal and delivers and distributes gas. In 2010, its market capitalization was around 15 billion Euros. Merck is the world's oldest operating chemical and pharmaceutical company with a market capitalization of 4 billion Euros in 2010. Plots of the daily and intradaily time evolution of price, volume, returns, and state of the LOB for each of the three stocks during our sample period can be found in the web-appendix. They reveal that our sample stocks did not exhibit any anomalous trading activity or biasing trend during the sample period.[9]

3. Procedure used for computing the risk measures

To compute the proposed risk measures, the model will first be estimated using deseasonalized data, and then the tests will be car-

[7] If market conditions change significantly, the model can, of course, be re-estimated.

[8] See Xetra Release 11.0—Enhanced Broadcast Solution and Interface Specification—for a detailed description.

[9] We thank an anonymous referee for suggesting this observation.

ried out on both deseasonalized and seasonalized data. Fig. 1 presents the flowchart of our methodology:

We now describe the main steps:

(a) We first compute the raw tick-by-tick durations defined as the time interval between two consecutive trades and tick-by-tick frictionless returns and actual returns based on the data of open LOB and trades.
(b) We further compute the frictionless return changes and actual return changes by taking the first difference of frictionless returns and actual returns, respectively. This step is required because the frictionless return and actual return are not time-additive and cannot be modeled directly.
(c) We remove seasonality from durations, frictionless return changes and actual return changes to obtain the corresponding deseasonalized data.
(d) The deseasonalized data are modeled by a LogACD-VARMA-MGARCH model.
(e) Once we have estimated the model, we simulate the deseasonalized data based on estimated coefficients and construct VaR measures at different confidence levels for backtesting on out-of-sample deseasonalized data.
(f) The seasonal factors are re-introduced into the deseasonalized data to generate the re-seasonalized data.
(g) As done in (e), we construct different quantiles for backtesting on out-of-sample re-seasonalized data.
(h) We construct impact coefficients of ex-ante liquidity risk based on the simulated re-seasonalized data.
(i) We further compute the IVaR and LIVaR, which are defined as the VaR for frictionless return and actual return, respectively.
(j) Based on the IVaR and LIVaR, we can finally compute the ex-ante liquidity premium by taking the ratio of the difference between LIVaR and IVaR over LIVaR.

The following sections will explain each step in detail.

4. Frictionless return, actual return and the corresponding high-frequency VaRs

We take into account all trading information that is available by modeling tick-by-tick data. The first characteristic in tick-by-tick data modeling is that the durations between two consecutive transactions are irregularly spaced. Consider two consecutive trades that arrive at t_{i-1} and t_i, and define dur_i as the duration from t_{i-1} to t_i. Based on this point process, we can further construct two return processes: frictionless return and actual return. More specifically, the frictionless return is defined as the log ratio of best bid price, $b_i(1)$ at moment i and previous best ask price, $a_{i-1}(1)$. The frictionless return is an ex-ante return indicating the tick-by-tick return for selling only one unit of stock.[10]

$$R_i^F = \ln\left(\frac{b_i(1)}{a_{i-1}(1)}\right). \tag{1}$$

The actual return is defined as the log ratio of selling price for a volume v and previous best ask price.[11]

$$R_i^B = \ln\left(\frac{b_i(v)}{a_{i-1}(1)}\right),$$

where

$$b_i(v) = \frac{\sum_{k=1}^{K-1} b_{k,i}v_{k,i} + b_{K,i}v_{K,i}}{v} \quad \text{and} \quad v_{K,i} = v - \sum_{k=1}^{K-1} v_{k,i}, \tag{2}$$

$b_{k,i}$ and $v_{k,i}$ are the kth level bid price and volume available, respectively. $v_{K,i}$ is the quantity left after $K-1$ levels are completely consumed by v. The consideration of quantity available in LOB is in line with other ex-ante liquidity measures in the market microstructure literature (Irvine et al., 2000; Domowitz et al., 2005; Coppejans et al., 2004, among others). The choice of volume v is motivated by transaction volume and volume available in LOB. Explicitly, for each stock we first compute the cumulative volume available over the 20 levels at each transaction moment for the bid side of LOB, and then we choose the minimum cumulative volume as the maximum volume to construct the actual returns. We thus avoid the situation where the actual price does not exist for a given volume. One concern that may arise involves iceberg orders, which keep a portion of the quantity invisible to market participants. In this study, we assume that the liquidity risk is faced by an impatient trader, and the possibility of trading against an iceberg order will not influence his trading behavior. According to Beltran-Lopez et al. (2009), the hidden part of the book does not carry economically significant informational content.[12] The difference between the frictionless return and the actual return is that the actual return takes into account the desired transaction volume, which is essential for the liquidity measure. Intuitively, the actual return measures the ex-ante return when liquidating v units of shares.

One characteristic of our defined frictionless returns and actual returns is that they do not possess the time-additivity property of traditional log-returns. To circumvent this difficulty, we model the frictionless return changes and actual return changes instead of modeling the actual return and frictionless return directly. More specifically, let $r_i^f = R_i^F - R_{i-1}^F$ and $r_i^b = R_i^B - R_{i-1}^B$ be the tick-by-tick frictionless return changes and actual return changes. Following this setup, the L-step forward frictionless return and actual return can be expressed as follows:

$$\begin{aligned} R_{i+L}^F &= \ln\left(\frac{b_{i+L}(1)}{a_{i+L-1}(1)}\right) = \ln\left(\frac{b_i(1)}{a_{i-1}(1)}\right) + r_{i+1}^f + r_{i+2}^f + \cdots r_{i+L}^f \\ &= R_i^F + \sum_{m=1}^{L} r_{i+m}^f, \end{aligned} \tag{3}$$

$$\begin{aligned} R_{i+L}^B &= \ln\left(\frac{b_{i+L}(v)}{a_{i+L-1}(1)}\right) = \ln\left(\frac{b_i(v)}{a_{i-1}(1)}\right) + r_{i+1}^b + r_{i+2}^b + \cdots r_{i+L}^b \\ &= R_i^B + \sum_{m=1}^{L} r_{i+m}^b, \end{aligned} \tag{4}$$

The terms $\sum_{m=1}^{L} r_{i+m}^f$ and $\sum_{m=1}^{L} r_{i+m}^b$ are the sum of all tick-by-tick changes in return over a predetermined interval and can be considered as the waiting cost related to frictionless returns and actual returns.[13] More specifically, they measure the costs/gains associated with the latter instead of immediate liquidation of one share and v shares of stock, respectively. Moreover, if we define the IVaR^c and LIVaR^c as the VaR for $\sum_{m=1}^{L} r_{i+m}^f$ and $\sum_{m=1}^{L} r_{i+m}^b$, respectively, and compute them for a predetermined time interval, then the IVaR^c and LIVaR^c will provide the maximal loss over a given interval and at a given confidence level for an investor that trades at frictionless or

[10] In the market microstructure literature, the mid-quote price is often used as a proxy for the unobserved efficient market price. However, from a practical perspective, traders can rarely obtain the mid-quote price during their transactions. Therefore, the use of the mid-quote price will underestimate the risk faced by active traders. We take a more realistic price, the best bid price, as the frictionless price for traders who want to liquidate their stock position.

[11] The frictionless return and actual return are defined similarly from buyers' viewpoint. This definition implicitly assumes that orders can be executed without any latency, and quote stuffing does not affect order execution.

[12] In our dataset, the hidden order information is not available.

[13] The waiting cost could be positive or negative, which indicates loss and gain, respectively.

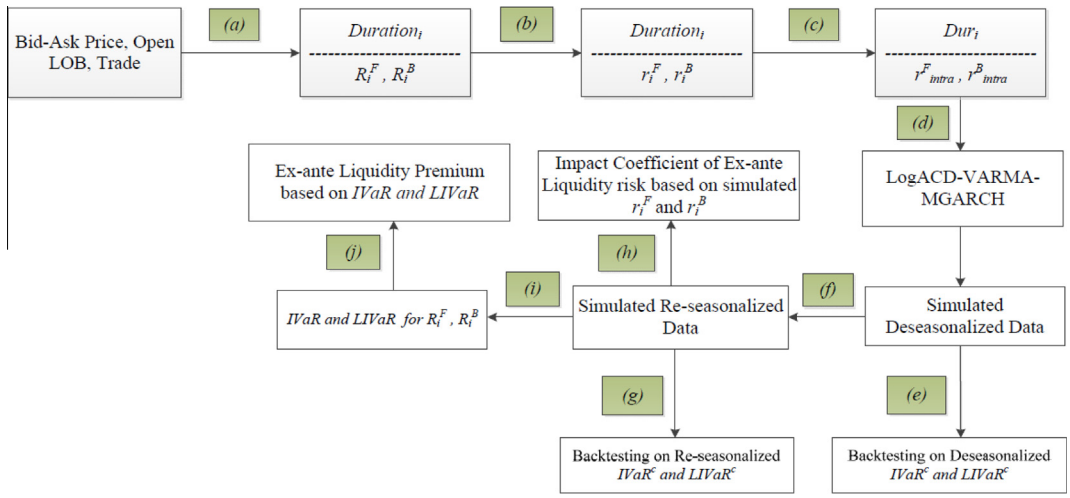

Fig. 1. Flowchart for computing impact coefficient of ex-ante liquidity risk and ex-ante liquidity premium. Shows the procedure we follow in this study: (a) Compute durations, frictionless returns and actual returns based on raw data; (b) Construct the frictionless return changes and actual return changes; (c) Remove seasonality from durations, frictionless return changes and actual return changes; (d) Estimate the model; (e) Backtest deseasonalized IVaR^c and LIVaR^c; (f) Compute the re-seasonalized data by re-introducing the seasonal factors; (g) Backtest re-seasonalized IVaR^c and LIVaR^c; (h) Compute the impact coefficient of ex-ante liquidity risk; (i) Compute the IVaR and LIVaR for frictionless return and actual return; (j) Derive the ex-ante liquidity risk premium.

actual return. In other words, the IVaR^c and LIVaR^c will estimate the maximal loss in terms of frictionless return and actual return, which are related to market risk and total risk (market risk and ex-ante liquidity risk), respectively. Mathematically, consider a realization of a sequence of intervals with length *int* and let $y^f_{int,t}$ and $y^b_{int,t}$[14] be the sum of tick-by-tick changes of returns r^f_j and r^b_j over the tth interval,

$$y^f_{int,t} = \sum_{j=\tau(t-1)}^{\tau(t)-1} r^f_j, \quad y^b_{int,t} = \sum_{j=\tau(t-1)}^{\tau(t)-1} r^b_j, \tag{5}$$

where $\tau(t)$ is the index for which the cumulative duration exceeds the tth interval with length *int* for the first time. By definition:

$$int \geqslant \sum_{j=\tau(t-1)}^{\tau(t)-1} dur_j \quad \text{and} \quad int \leqslant \sum_{j=\tau(t-1)}^{\tau(t)} dur_j. \tag{6}$$

The process of duration allows us to aggregate the tick-by-tick data to construct the dynamics of frictionless return and actual return for a predetermined interval that allows consideration of risk in calendar time. Accordingly, the IVaR^c and LIVaR^c[15] for frictionless return changes and actual return changes with confidence level $1-\alpha$ for a predetermined interval *int* are defined as:

$$Pr\left(y^f_{int,t} < IVaR^c_{int,t}(\alpha)|I_t\right) = \alpha;$$

$$Pr\left(y^b_{int,t} < LIVaR^c_{int,v,t}(\alpha)|I_t\right) = \alpha,$$

I_t is the information set until moment $\tau(t-1)$. Similar to the traditional definition of VaR, $IVaR^c_{int,t}(\alpha)$ and $LIVaR^c_{int,v,t}(\alpha)$ are the conditional α-quantiles for $y^f_{int,t}$ and $y^b_{int,t}$.

We can further define the IVaR and LIVaR as the VaR for the frictionless return and actual return as follows: $IVaR_{int,t} = R^F_{\tau(t-1)} + IVaR^c_{int,t}$,

$$LIVaR_{int,v,t} = R^B_{\tau(t-1)} + LIVaR^c_{int,v,t},$$

where $R^F_{\tau(t-1)}$ and $R^B_{\tau(t-1)}$ are the frictionless return and actual return at the beginning of the tth interval. Consequently, IVaR and LIVaR estimate the α-quantiles for frictionless return and actual return at the end of the t-th interval.

5. Methodology

In our tick-by-tick modeling, there are three random processes: duration, changes in the frictionless return and changes in the actual return. The present study assumes that the duration evolution is strongly exogenous but has an impact on the volatility of frictionless and actual return changes. The joint distribution of duration, frictionless return change and actual return change can be decomposed into the marginal distribution of duration and joint distribution of frictionless and actual return change conditional on duration. More specifically, the joint distribution of the three variables is:

$$\begin{aligned} &f^{d,f,b}\left(dur_i, r^f_i, r^b_i \middle| dur_{i-1}, r^f_{i-1}, r^b_{i-1}; \Theta^f\right) \\ &= f^d\left(dur_i \middle| dur_{i-1}, r^f_{i-1}, r^b_{i-1}; \theta^d\right) f^{f,b}\left(r^f_i, r^b_i \middle| dur_i, dur_{i-1}, r^f_{i-1}, r^b_{i-1}; \theta^d, \theta^{f,b}\right), \end{aligned} \tag{7}$$

where $f^{d,f,b}$ is the joint distribution for duration, frictionless return change and actual return change. $f^d(\cdot)$ is the marginal density for duration and $f^{f,d}(\cdot)$ is the joint density for actual and frictionless return changes. Consequently, the corresponding log-likelihood function for each joint distribution can be written as:

$$\begin{aligned} L(\theta^d, \theta^{f,b}) = &\sum_{i=1}^{n} \log f^d\left(dur_i \middle| dur_{i-1}, r^f_{i-1}, r^b_{i-1}; \theta^d\right) \\ &+ \log f^{f,b}\left(r^f_i, r^b_i \middle| dur_{i-1}, r^f_{i-1}, r^b_{i-1}, dur_i; \theta^{f,b}\right), \end{aligned} \tag{8}$$

[14] y^f_{int} and y^b_{int} are defined on both seasonalized return changes and deseasonalized return changes.

[15] IVaR^c and LIVaR^c are also defined on both seasonalized return changes and deseasonalized return changes. Moreover, our IVaR^c and LIVaR^c can also be used in the strategy of short selling where IVaR^c and LIVaR^c will be the $1-\alpha$ quantiles of the distributions.

In the next subsections, we specify marginal density for dynamics of duration and joint density for frictionless return and actual return changes. We present the model for deseasonalized duration, frictionless and actual return changes. The deseasonalization procedure is described in detail in the web-appendix.

5.1. Model for duration

The ACD model used to estimate the duration between two consecutive transactions was introduced by Engle and Russell (1998). The GARCH-style structure is used to capture the duration clustering observed in high-frequency financial data. The basic assumption is that the realized duration is driven by its conditional duration and a positive random variable as an error term. Let $\psi_i = E(dur_i|I_{i-1})$ be the expected duration given all the information up to $i-1$, and ε_i be the positive random variable. The duration can be expressed as: $dur_i = \psi_i \cdot \varepsilon_i$. There are several possible specifications for the expected duration and the independent and identically distributed (i.i.d.) positive random error (see Hautsch, 2004; Pacurar, 2008 for surveys). To guarantee the positivity of duration, we adopt the log-ACD model proposed by Bauwens and Giot (2000). The specification for expected duration is

$$\psi_i = \exp\left(\omega + \sum_{j=1}^{p}\alpha_j\varepsilon_{i-j} + \sum_{j=1}^{q}\beta_j \ln\psi_{i-j}\right). \tag{9}$$

For positive random errors, we use the generalized gamma distribution, which allows a non-monotonic hazard function and nests the Weibull distribution (Grammig and Maurer, 2000; Zhang et al., 2001):

$$p(\varepsilon_i|\gamma_1,\gamma_2) = \begin{cases} \frac{\gamma_1 \varepsilon_i^{\gamma_1\gamma_2-1}}{\gamma_3^{\gamma_1\gamma_2}\Gamma(\gamma_2)} \exp\left[-\left(\frac{\varepsilon_i}{\gamma_3}\right)^{\gamma_1}\right], & \varepsilon_i > 0, \\ 0, & \text{otherwise.} \end{cases} \tag{10}$$

where $\gamma_1, \gamma_2 > 0$, $\Gamma(\cdot)$ is the gamma function, and $\gamma_3 = \Gamma(\gamma_2)/\Gamma\left(\gamma_2 + \frac{1}{\gamma_1}\right)$.

5.2. Model for frictionless return and actual return changes

The high-frequency frictionless return and actual return changes display a high serial correlation. To capture this microstructure effect, we follow Ghysels and Jasiak (1998) and adopt a VARMA (p,q) structure:

$$\begin{aligned} &R_i = \left(r_i^b, r_i^f\right)', E_i = \left(e_i^b, e_i^f\right)', \\ &R_i = \sum_{m=1}^{p}\Phi_m R_{i-m} + E_i - \sum_{n=1}^{q}\Delta_n E_{i-n}, \end{aligned} \tag{11}$$

where Φ_m and Δ_n are matrices of coefficients for R_{i-m} and E_{i-n}, respectively. As mentioned in Dufour and Pelletier (2011), we cannot directly work with the representation in (11) because of an identification problem. Consequently, we impose the restrictions on Δ_n by supposing that the VARMA representation is in diagonal MA form. More specifically, $\Delta_n = \begin{pmatrix} \delta_{11}^{(n)} & 0 \\ 0 & \delta_{22}^{(n)} \end{pmatrix}$ where $\delta_{11}^{(n)}$ and $\delta_{22}^{(n)}$ are the coefficients for nth-lag error terms of the actual return change and frictionless return change, respectively.

Furthermore, we assume the volatility part follows a multivariate GARCH process:

$$\begin{pmatrix} e_i^b \\ e_i^f \end{pmatrix} = H_i^{1/2} z_i,$$

where z_i is the bivariate normal distribution that has the following two moments: $E(z_i) = 0$, $Var(z_i) = I_2$. The normality assumption for the error term is supported by backtesting. The other distributions we tried, such as Normal Inverse Gaussian (NIG), Student-t and Johnson, overestimated the error distribution in our simulation tests.

H_i is the conditional variance matrix for R_i that should be positive-definite. To model the dynamic of H_i, we use the DCC structure proposed by Engle (2002) in which H_i is decomposed as follows:

$$\begin{aligned} &H_i = D_i C_i D_i, \\ &\text{where :} \\ &\begin{cases} D_i = diag\left(\sqrt{h_{11i}}, \sqrt{h_{22i}}\right), h_{11i} = \sigma_{11i}^2 dur_i^{\gamma_b}, h_{22i} = \sigma_{22i}^2 dur_i^{\gamma_f}, \\ C_i = (diagQ_i)^{-1/2} Q_i (diagQ_i)^{-1/2}, \end{cases} \end{aligned}$$

and

$$\begin{aligned} &Q_i = (1-\theta_1-\theta_2)Q + \theta_1 \varepsilon_{i-1}\varepsilon_{i-1}' + \theta_2 Q_{i-1}, \quad \varepsilon_{k,i-1} = \frac{e_{k,i-1}}{\sqrt{h_{kk,i-1}}}, \\ &k = 1,2, \end{aligned} \tag{12}$$

Q is the unconditional correlation matrix of $\{\varepsilon_i\}_{i=1}^N$, $\sqrt{h_{11i}}\left(\sqrt{h_{22i}}\right)$ is the conditional variance for actual (frictionless) return change, and $\gamma_b(\gamma_f)$ measures the impact of duration on the volatilities of actual and frictionless return changes, respectively.[16]

In the DCC framework, each series has its own conditional variance. For both actual and frictionless return changes, we adopt a NGARCH(m,n) (Nonlinear GARCH) process as proposed by Engle and Ng (1993) to capture the cluster as well as the asymmetry in volatility. The process can be written as:

$$\begin{aligned} &h_{11,i} = \sigma_{11,i}^2 \cdot dur_i^{\gamma_b}, \\ &\sigma_{11,i}^2 = \omega^b + \sum_{j=1}^{m}\alpha_j^b \sigma_{11,i-j}^2 + \sum_{j=1}^{n}\beta_j^b \sigma_{11,i-j}^2 \left(\varepsilon_{i-j}^b - \pi^b\right)^2, \end{aligned} \tag{13}$$

and

$$\begin{aligned} &h_{22,i} = \sigma_{22,i}^2 \cdot dur_i^{\gamma_f}, \\ &\sigma_{22,i}^2 = \omega^f + \sum_{j=1}^{m}\alpha_j^f \sigma_{22,i-j}^2 + \sum_{j=1}^{n}\beta_j^f \sigma_{22,i-j}^2 (\varepsilon_{i-j}^f - \pi^f)^2, \end{aligned} \tag{14}$$

where π^b and π^f are used to capture the asymmetry in the conditional volatilities. When π^f or $\pi^b = 0$, the model will become a standard GARCH model, whereas a negative π^f or π^b indicates that a negative shock will cause higher conditional volatilities for the next moment. Our structure also explicitly introduces the duration dimension in conditional volatilities. In his pioneering study of the impact of duration on volatility, Engle (2000) assumes that the impact is linear, that is, $h_{11i} = \sigma_{11,i}^2 \cdot dur_i$. This modeling for the unit of time might be restrictive for some empirical data for which conditional volatility can depend on duration in a more complicated way. To make the model more general, we follow Dionne et al. (2009) by assuming the power form $h_{11,i} = \sigma_{11,i}^2 \cdot dur_i^{\gamma_b}$ and $h_{22,i} = \sigma_{22,i}^2 \cdot dur_i^{\gamma_f}$. When γ_f or $\gamma_b = 0$, the volatility will become a standard NGARCH process, whereas when γ_f or $\gamma_b = 1$, it transforms to the similar model studied in Engle (2000).

As mentioned above, our model has three uncertainties: duration uncertainty, price uncertainty and LOB uncertainty. Deriving a closed form of LIVaR^c would be complicated for multi-period

[16] The DCC model can be estimated by a two-step approach. Engle and Sheppard (2001) show that the likelihood of the DCC model can be written as the sum of two parts: a mean and volatility part, and a correlation part. Even though the estimators from the two-step estimation are not fully efficient, the one iteration of a Newton–Raphson algorithm applied to total likelihood provides asymptotically efficient estimators.

forecasting in the presence of three risks, especially for non-regular time duration. Therefore, once the models are estimated, we follow Christoffersen (2003) and use Monte Carlo simulations to make multi-step forecasts and to test the model's performance.

6. Empirical results

6.1. Seasonality adjustment

It is well known that high-frequency data behave very differently from low-frequency data. Tables 1.1–1.3 present the descriptive statistics of raw and deseasonalized duration, frictionless return changes and actual return changes for which various volumes are chosen for the three studied stocks. From Panels A, we can observe that for the sample period (the first two weeks of July 2010), SAP is the most liquid stock: the average duration is the shortest and the number of observations is the largest. MRK is the least liquid one. Moreover, given that the variables are constructed on tick-by-tick frequency, all three stocks have an average of zero and a very small standard deviation for frictionless return changes and actual return changes. All three stocks present high kurtosis due to the fact that most of the observations are concentrated on their average and co-exist with some extreme values. In addition, the raw data are characterized by extremely high autocorrelation for both first and second moments for all of the variables.

High-frequency data are characterized by seasonality (Anatolyev and Shakin, 2007; Andersen and Bollerslev, 1997; Dufour and Engle, 2000), which should be removed before estimating any model. We follow an approach similar to Dionne et al. (2009) by using a two-step deseasonalization procedure, interday and intraday.

Supplementary Fig. A1 in the web-appendix illustrates the evolution of the seasonality factors of RWE for duration, frictionless and actual return changes when $v = 4000$ shares.[17] It is not surprising to see that the frictionless and actual return changes have similar dynamics because the actual return changes contain the frictionless return changes. However, the magnitude for frictionless and actual return changes differs. Panels B of Tables 1.1–1.3 report descriptive statistics of deseasonalized durations, frictionless and actual return changes. The raw frictionless and actual return changes have been normalized to bring the mean to zero and standard deviation to one. However, other statistics such as skewness, kurtosis and auto-correlation are not affected by this normalization process. The high kurtosis and auto-correlation will be captured by the proposed models.

6.2. Estimation results

We use the model presented in Section 5 to fit SAP, RWE and MRK deseasonalized data. The estimation data cover the first week of July 2010. The data from the second week are used as out-of-sample data to test the model's performance. As previously mentioned, the estimation is realized jointly for frictionless and actual return changes. The likelihood function is maximized using Matlab v7.6.0 with Optimization toolbox.

Tables 2.1–2.3 report the estimation results for actual return changes for SAP, RWE and MRK for $v = 4000$, 4000 and 1800 shares, respectively. It should be noted that for each stock, the frictionless return changes and actual return changes are governed by the same duration process, which is assumed to be strictly exogenous. The high clustering phenomenon is indicated in deseasonalized data by the Ljung–Box statistic (see Tables 1.1–1.3 Panel B). The clustering in duration is confirmed by the Log-ACD model. The better fits of the data are obtained with a Log-ACD(2,1) specification for SAP durations, a Log-ACD(3,1) model for RWE durations and a Log-ACD(1,1) model for MRK durations. The Ljung–Box statistic on standardized residuals of duration provides evidence that the Log-ACD model is capable of removing the high autocorrelation identified in deseasonalized duration data. The Ljung–Box statistic with 15 lags is dramatically reduced to 25.08 for SAP, 39.7 for RWE and 21.79 for MRK.

Frictionless and actual return changes of the three stocks are also characterized by a high autocorrelation in level and volatility. Moreover, the Ljung–Box statistics with 15 lags on deseasonalized return change and its volatility reject independence at any significance level for the three stocks. Taking the model efficiency and parsimony into consideration, the better fits of the data are obtained with a VARMA(4,2)-MGARCH((1,3),(1,3))[18] model for SAP, a VARMA(5,1)-MGARCH((1,3),(1,3)) model for RWE and the specification of VARMA(2,2)-MGARCH((1,3),(1,3)) for MRK. The model adequacy is assessed based on standardized residuals and squared standardized residuals. Taking MRK as an example, the Ljung-Box statistics for standardized residuals and squared standardized residuals of actual return changes, computed with 5, 10, 15, 20 lags, respectively, are not significant at the 5% level. The Ljung–Box statistic with 15 lags has been significantly reduced after modeling to 7.72. Similar results are obtained for stocks RWE and SAP.

Regarding the estimated parameters, the sum of coefficients in each individual GARCH model is close to one, indicating a high persistence in volatility. Further, π^f and π^b are significantly different from zero in both structures, thus evidencing asymmetric effects. In other words, a negative shock generates a higher conditional volatility for the next moment. It also should be noted that γ_b and γ_f are both positive for the three stocks. This means that a longer duration will generate higher volatility for both actual return and frictionless return changes. In addition, due to the fractional exponent, volatility increases slowly as duration lengthens. In our model, volatility is the product of no-duration scaled variance and duration factor, and the γ_b of actual return changes are higher than γ_f of frictionless return changes for the three stocks. This implies that the duration factor has a larger impact on actual returns than on frictionless returns.

The use of dynamic conditional correlation is justified by the fact that θ_1 and θ_2 in Eq. (12) are both significantly different from zero for the three stocks. As expected, the conditional correlation of actual return and frictionless return changes is time-varying. A sum of the two parameters of around 0.8 confirms the high persistence of conditional correlation.

6.3. Model performance and backtesting

In this section, we present the simulation procedure and backtesting results on simulated deseasonalized and re-seasonalized frictionless and actual return changes. Once the model is estimated on tick-by-tick frequency, we can test the model performance and compute frictionless $IVaR^c$ and $LIVaR^c$ by Monte Carlo simulation. One of the advantages of our method is that once the model is estimated, we can compute the simulated deseasonalized $IVaR^c$ and $LIVaR^c$ for any horizon without re-estimating the model. In addition, we can compute the simulation-based re-seasonalized $IVaR^c$ and $LIVaR^c$ in traditional calendar time using the available seasonal factors.

We choose different time intervals to test the model performance. The interval lengths are 40, 50, 60, 80, 100, 120 and 140 units of time for the more liquid stocks SAP and RWE and 20, 30, 40, 50, 60, 80 and 100 for the less liquid stock MRK. Given that

[17] Results on other volumes for RWE, SAP and MRK are available upon request.

[18] NGARCH(1,3) for actual return changes and NGARCH(1,3) for frictionless return changes.

Table 1.1
Descriptive statistics for SAP raw and deseasonalized data.

	Mean	Std. Dev.	Skew	Kurt	Min	Max	LB(15)	LB2(15)
Panel A: SAP raw data								
Duration	6.43	13.21	4.58	37.28	1.00E−03	292.75	6909.93	1426.06
FR change	6.39E−09	1.93E−04	0.10	6.01	−1.98E−03	1.47E−03	6408.48	7082.94
AR (v = 8000)	−7.77E−09	1.66E−04	0.13	8.13	−1.92E−03	2.14E−03	5096.10	6512.58
AR (v = 6000)	−6.25E−09	1.66E−04	0.10	7.43	−1.93E−03	1.72E−03	5252.56	6021.21
AR (v = 4000)	−4.73E−09	1.68E−04	0.09	7.79	−1.96E−03	2.11E−03	5374.51	5185.26
AR (v = 2000)	−2.76E−09	1.72E−04	0.11	7.15	−1.98E−03	1.90E−03	5514.05	5156.26
Panel B: SAP deseasonalized data								
Duration	1.00	1.88	4.21	37.82	0.00	52.68	4345.54	1528.45
FR change	−1.33E−04	1.01	0.07	5.99	−10.96	7.21	6411.40	5923.61
AR (v = 8000)	−4.32E−05	1.04	0.08	9.99	−15.37	11.25	5043.46	6599.80
AR (v = 6000)	−1.05E−05	1.04	0.08	9.45	−13.07	12.60	5184.79	7189.66
AR (v = 4000)	−6.65E−05	1.03	0.07	8.33	−12.78	10.76	5324.84	5661.21
AR (v = 2000)	−1.37E−04	1.02	0.09	7.26	−12.78	9.69	5501.73	4684.47

The table shows the descriptive statistics for raw durations, actual return changes when Q = 2000, 4000, 6000, 8000 and frictionless return changes. The sample period is the first 2 weeks of July 2010 with 44,467 observations.

Table 1.2
Descriptive statistics for RWE raw and deseasonalized data.

	Mean	Std.Dev.	Skew	Kurt	Min	Max	LB(15)	LB2(15)
Panel A: RWE raw data								
Duration	7.64	15.88	4.75	37.53	1.00E−03	296.58	10061.17	2479.01
FR change	−3.10E−08	2.51E−04	0.12	7.51	−3.07E−03	2.49E−03	5091.89	7971.04
AR (v = 4000)	−4.33E−08	2.23E−04	0.22	10.01	−2.96E−03	2.38E−03	3940.66	10253.80
AR (v = 3000)	−4.05E−08	2.25E−04	0.18	10.00	−3.29E−03	2.37E−03	4022.16	10239.86
AR (v = 2000)	−3.70E−08	2.27E−04	0.18	9.19	−3.22E−03	2.33E−03	4131.99	10306.19
AR (v = 1000)	−3.12E−08	2.32E−04	0.16	8.75	−3.19E−03	2.42E−03	4364.74	11046.85
Panel B: RWE deseasonalized data								
Duration	0.97	1.73	3.71	24.51	2.45E−05	28.63	3101.10	577.62
FR change	−7.80E−05	0.98	0.12	6.00	−8.55	7.80	5123.94	5093.30
AR (v = 4000)	−1.23E−04	0.99	0.20	7.32	−8.61	10.11	3930.82	4781.76
AR (v = 3000)	−1.13E−04	0.98	0.18	7.08	−9.52	9.60	4002.22	4796.94
AR (v = 2000)	−1.01E−04	0.98	0.17	6.66	−9.40	9.14	4101.41	4888.15
AR (v = 1000)	−8.61E−05	0.98	0.17	6.38	−9.27	8.52	4315.98	5519.57

The table shows the descriptive statistics for raw durations, actual return changes when Q = 1000, 2000, 3000, 4000 and frictionless return changes. The sample period is the first 2 weeks of July 2010 with 37,394 observations.

Table 1.3
Descriptive statistics for MRK raw and deseasonalized data.

	Mean	Std.Dev.	Skew	Kurt	Min	Max	LB(15)	LB2(15)
Panel A: MRK raw data								
Duration	16.31	36.40	5.16	47.06	0.001	718.35	2157.42	905.39
FR change	−3.83E−09	3.11E−04	0.00	15.52	−5.03E−03	4.25E−03	2551.10	4125.30
AR (v = 2700)	−1.33E−08	2.74E−04	−0.02	24.71	−4.71E−03	3.75E−03	1672.50	2303.16
AR (v = 1800)	−9.58E−09	2.79E−04	0.17	24.70	−4.77E−03	4.74E−03	1754.34	2308.44
AR (v = 900)	−6.82E−09	2.84E−04	0.24	21.74	−4.82E−03	4.50E−03	1890.60	3030.64
Panel B: MRK deseasonalized data								
Duration	0.97	1.95	4.13	29.42	1.581E−05	26.65	736.41	150.75
FR change	−2.55E−04	1.01	0.06	13.44	−13.87	11.61	2537.61	4884.19
AR (v = 2700)	−2.78E−04	1.03	0.14	15.67	−14.65	11.65	1670.95	2537.68
AR (v = 1800)	−2.81E−04	1.03	0.20	17.60	−14.15	15.63	1730.01	2201.63
AR (v = 900)	−2.68E−04	1.02	0.33	16.44	−13.79	16.86	1862.13	2289.72

The table shows the descriptive statistics for raw durations, actual return changes when Q = 900, 1800, 2700 and frictionless return changes. The sample period is the first 2 weeks of July 2010 with 17,472 observations.

the model is applied to deseasonalized data, the simulated duration is not in calendar units. However, simulated duration and calendar time intervals are related in a proportional way. Further, depending on the trading intensity, the simulated duration does not correspond to the same calendar time interval. For a more liquid stock, the same simulated interval relates to a shorter calendar time interval. For instance, in the case of MRK, the interval length 50 re-samples the one-week data for 190 intervals and corresponds to 13.42 min, and the interval-length relates 100 to 95 intervals and corresponds to 26.84 min. However, for a more liquid stock such as SAP, the interval-length 50 corresponds to 5.45 min and the interval-length 140 corresponds to 15.27 min.

The simulations for frictionless and actual return changes are realized as follows:

(1) We generate the duration between two consecutive transactions and assume that the duration process is strongly exogenous.

Table 2.1
Estimation results SAP ($v = 4000$).

Estimation log-ACD(2,1)-VARMA(4.2)-NGARCH((1.3).(1.3)) (Obs = 21089)						
ACD(2.1)	Parameters	Estimation	Std error	Statistics		
	α_1	0.127	0.009	LB test on residuals		
	α_2	−0.049	0.009	Lags	Statistic	C_Value
	β_1	0.963	0.004	5	5.364	11.070
	γ_1	0.812	0.022	10	13.045	18.307
	γ_2	0.419	0.016	15	**25.077**	24.996
	ω	−0.081	0.004	20	30.561	31.410
Actual return changes VARMA(4.2)-NGARCH((1.3).(1,3))	$\varphi_{11}^{(1)}$	1.043	0.088			
	$\varphi_{12}^{(1)}$	−0.322	0.010			
	$\varphi_{11}^{(2)}$	−0.154	0.061			
	$\varphi_{12}^{(2)}$	0.089	0.031	5	5.291	11.070
	$\varphi_{11}^{(3)}$	−0.031	0.016	10	13.424	18.307
	$\varphi_{12}^{(3)}$	0.047	0.014	15	16.106	24.996
	$\varphi_{11}^{(4)}$	0.032	0.011	20	18.769	31.410
	$\varphi_{12}^{(4)}$	**0.008**	**0.012**	LB test on squared residuals		
	$\delta_{11}^{(1)}$	−1.338	0.087			
	$\delta_{11}^{(2)}$	0.353	0.085	Lags	Statistic	C_Value
	ω^b	0.088	0.004	5	3.395	11.070
	α_1^b	0.412	0.022	10	15.405	18.307
	β_1^b	0.159	0.006	15	18.925	24.996
	π^b	0.404	0.022	20	21.266	31.410
	α_3^b	0.308	0.018			
	γ^b	0.073	0.002			
Frictionless return changes ARMA(4,2)-GARCH((1,3),(1,3))	$\varphi_{22}^{(1)}$	0.6055	0.0693	LB test on residuals		
	$\varphi_{21}^{(1)}$	0.1754	0.0093			
	$\varphi_{22}^{(2)}$	−0.0401	0.0175	Lags	Statistic	C_Value
	$\varphi_{21}^{(2)}$	−0.0593	0.0187	5	**15.811**	11.070
	$\varphi_{22}^{(3)}$	0.0488	0.0133	10	**21.046**	18.307
	$\varphi_{21}^{(3)}$	−0.0199	0.0103	15	23.203	24.996
	$\delta_{22}^{(1)}$	−1.4122	0.0690	20	**32.595**	31.410
	$\delta_{22}^{(2)}$	0.4265	0.0669	LB test on squared residuals		
	ω^f	0.0716	0.0037			
	α_1^f	0.4799	0.0305	Lags	Statistic	C_Value
	β_1^f	0.1612	0.0074	5	7.794	11.070
	π^f	0.3466	0.0254	10	17.916	18.307
	α_3^f	0.2472	0.0237	15	21.902	24.996
	γ^f	0.0377	0.0025	20	24.743	31.410
DCC parameter	θ_1	0.0791	0.0032			
	θ_2	0.7537	0.0113			

The statistics column reports the Ljung–Box statistic on standardized residuals of duration, actual return changes and squared standardized residuals for different lags. The bold entries are the estimation coefficients that are not significantly different from zero and the Ljung–Box statistics that reject the non-correlation in the residuals.

(2) With the simulated duration and estimated coefficients of the VARMA-MGARCH model, we obtain the corresponding return changes.
(3) We repeat steps 1 and 2 for 10,000 paths and re-sample the data at each path according to the predetermined interval.
(4) For each interval, we compute the corresponding $IVaR^c$ and $LIVaR^c$ at the desired level of confidence. To conduct the backtesting for each given interval, we also need to construct the return changes for original out-of-sample data.

To validate the model, we conduct the unconditional coverage and independence tests by applying the Kupiec test (1995), the Christoffersen test (1998), and the recently proposed tests of Ziggel et al. (2014). The Kupiec test checks whether the empirical failure rate is statistically different from the failure rate we are testing, whereas the Christoffersen test evaluates the independence aspect of the violations. More specifically, it rejects VaR models that generate clustered violations by estimating a first-order Markov chain model on the sequence. The new set of tests proposed by Ziggel et al. (2014) analyze unconditional coverage and independence by using simulations with i.i.d Bernoulli random variables. One advantage is that the new tests allow for two-sided testing. Table 3 reports the p-values for all tests (two-sided testing for unconditional coverage and i.i.d) on simulated data for confidence levels of 95%, 97.5%, 99% and 99.5%. The time interval varies from 5 min to 15 min for SAP, from 5 min to 16.67 min for RWE and from 5 min to 27 min for MRK. Most of the p-values are higher than 5%, indicating that the model generally captures the distribution of frictionless and actual return changes well.

Because most trading and risk management decisions are based on calendar time and raw data, it might be difficult for practitioners to use simulated deseasonalized data to conduct risk management. To this end, we conduct another Monte Carlo simulation that takes into account the time-varying deterministic seasonality factors. The process is similar to that used for simulating deseasonalized data. However, the difference is that we re-introduce the seasonality factors for duration, actual return changes and frictionless return

Table 2.2
Estimation results RWE ($v = 4000$).

Estimation log-ACD(3,1) VARMA(5.1)- NGARCH((1.3).(1.3)) (Obs = 15,320)						
ACD(3.1)	Parameter	Estimation	Std error	Statistics		
	α_1	0.108	0.010	LB test on residuals		
	α_2	−0.020	0.013			
	α_3	−0.024	0.009	Lags	Statistic	C_Value
	β_1	0.970	0.004	5	9.209	11.070
	γ_1	1.145	0.028	10	**20.280**	18.307
	γ_2	0.280	0.010	15	**39.712**	24.996
	ω	−0.068	0.004	20	**44.304**	31.410
Actual return changes VARMA(5.1)-NGARCH((1.3).(1,3))	$\varphi_{11}^{(1)}$	0.710	0.012			
	$\varphi_{12}^{(1)}$	−0.333	0.011			
	$\varphi_{11}^{(2)}$	0.047	0.014			
	$\varphi_{12}^{(2)}$	**0.005**	**0.013**			
	$\varphi_{11}^{(3)}$	**0.006**	**0.014**	5	10.161	11.070
	$\varphi_{12}^{(3)}$	0.024	0.013	10	14.653	18.307
	$\varphi_{11}^{(4)}$	0.006	0.014	15	**27.042**	24.996
	$\varphi_{12}^{(4)}$	**0.009**	**0.013**	20	30.095	31.410
	$\varphi_{11}^{(5)}$	0.041	0.012	LB test on squared residuals		
	$\varphi_{12}^{(5)}$	**0.007**	**0.012**			
	$\delta_{11}^{(1)}$	−0.980	0.002			
	ω^b	0.099	0.006	Lags	Statistic	C_Value
	α_1^b	0.437	0.030	5	4.356	11.070
	β_1^b	0.156	0.008	10	8.474	18.307
	π^b	0.461	0.029	15	11.071	24.996
	α_3^b	0.260	0.023	20	14.102	31.410
	γ^b	0.067	0.003			
Frictionless return changes VARMA(5.1)-NGARCH((1.3).(1,3))	$\varphi_{22}^{(1)}$	0.2324	0.0123			
	$\varphi_{21}^{(1)}$	0.1447	0.0109	LB test on residuals		
	$\varphi_{22}^{(2)}$	0.0374	0.0132			
	$\varphi_{21}^{(2)}$	**0.0048**	**0.0131**	Lags	Statistic	C_Value
	$\varphi_{22}^{(3)}$	0.0746	0.0135	5	6.378	11.070
	$\varphi_{21}^{(3)}$	−0.0428	0.0133	10	9.420	18.307
	$\varphi_{22}^{(4)}$	0.0305	0.0138	15	13.824	24.996
	$\varphi_{21}^{(4)}$	−**0.0168**	**0.0132**	20	22.560	31.410
	$\varphi_{22}^{(5)}$	**0.0205**	**0.0128**			
	$\varphi_{21}^{(5)}$	0.0179	0.0114			
	$\delta_{22}^{(1)}$	−0.9805	0.0018	LB test on squared residuals		
	ω^f	0.0711	0.0049			
	α_1^f	0.4586	0.0343	Lags	Statistic	C_Value
	β_1^f	0.1436	0.0080	5	7.403	11.070
	π^f	0.4531	0.0359	10	16.284	18.307
	α_3^f	0.2731	0.0276	15	19.750	24.996
	γ^f	0.0299	0.0029	20	22.811	31.410
DCC parameter	θ_1	0.0813	0.0043			
	θ_2	0.7791	0.0135			

The statistics column reports the Ljung–Box statistic on standardized residuals of duration, actual return changes and squared standardized residuals for different lags. The bold entries are the estimation coefficients that are not significantly different from zero and the Ljung–Box statistics that reject the non-correlation in the residuals.

changes. Given that seasonality factors vary from one day to another, the simulation should take the day of week into account. More precisely, for the first day, simulated durations are converted to a calendar time of that day and the corresponding timestamp identifies seasonality factors for actual and frictionless return changes. The simulation process continues until the corresponding timestamp surpasses the closing time for the underlying day. In the case of a multiple-day simulation, the process continues for another day. Based on the simulated re-seasonalized data, we also compute our $IVaR^c$ and $LIVaR^c$ by repeating the same algorithm.

Table 4 presents the backtesting results on the re-seasonalized simulated data. The time interval varies from 5 min to 10 min for the three stocks, and the confidence levels to test are 95%, 97.5%, 99% and 99.5%. Similar to the test results for simulated deseasonalized data, the p-values suggest that the simulated re-seasonalized data also provide reliable high-frequency risk measures for all chosen confidence levels over intervals of 5–10 min.

7. Risks for waiting cost, ex-ante liquidity risk and various IVaRs

7.1. Risks for waiting cost

As shown in Section 4, the sums of tick-by-tick frictionless return changes and actual return changes over a given interval can be viewed as the waiting costs related to market risk and total risk, which contains market risk and ex-ante liquidity risk. Consequently, the corresponding $IVaR^c$ and $LIVaR^c$ estimate the risk of losses on these waiting costs. Based on simulated re-seasonalized data from the previous section that contain the

Table 2.3
Estimation results MRK ($\upsilon = 1800$).

Estimation log-ACD(1,1)-VARMA(1.1)-NGARCH((1.3).(1.3)) (Obs = 7653)						
ACD(1.1)	Parameter	Estimation	Std error	Statistics		
				LB test on residuals		
	α_1	0.048	0.005	Lags	Statistic	C_Value
	β_1	0.984	0.004	5	8.240	11.070
	γ_1	0.784	0.034	10	17.239	18.307
	γ_2	0.382	0.025	15	21.796	24.996
	ω	−0.049	0.005	20	25.006	31.410
Actual return changes VARMA(2.2)-NGARCH((1.3).1)	$\varphi_{11}^{(1)}$	0.9401	0.0599			
	$\varphi_{12}^{(1)}$	−0.3679	0.0149			
	$\varphi_{11}^{(2)}$	**−0.0316**	**0.0515**	5	**11.971**	11.070
	$\varphi_{12}^{(2)}$	0.0945	0.0264	10	**25.105**	18.307
	$\delta_{11}^{(1)}$	−1.1788	0.0584	15	**27.396**	24.996
	$\delta_{11}^{(2)}$	0.2028	0.0565	20	29.201	31.410
	ω^b	0.1543	0.0109	LB test on squared residuals		
	α_1^b	0.3863	0.0341	Lags	Statistic	C_Value
	β_1^b	0.1877	0.0115	5	1.818	11.070
	π^b	0.4853	0.0328	10	3.084	18.307
	α_3^b	0.2238	0.0289	15	7.719	24.996
	γ^b	0.0861	0.0032	20	10.320	31.410
Frictionless return changes ARMA(1,3)-GARCH((1,3),1)	$\varphi_{22}^{(1)}$	0.4737	0.0725	LB test on residuals		
	$\varphi_{21}^{(1)}$	0.1822	0.0129	Lags	Statistic	C_Value
	$\varphi_{22}^{(2)}$	0.0422	0.0228	5	**20.248**	11.070
	$\varphi_{21}^{(2)}$	−0.0652	0.0179	10	**28.844**	18.307
	$\delta_{22}^{(1)}$	−1.2728	0.0712	15	**30.197**	24.996
	$\delta_{22}^{(2)}$	0.3020	0.0677	20	**34.977**	31.410
	ω^f	0.1551	0.0119	LB test on squared residuals		
	α_1^f	0.4034	0.0378	Lags	Statistic	C_Value
	β_1^f	0.2373	0.0163	5	4.348	11.070
	α_3^f	0.1670	0.0272	10	11.419	18.307
	γ^f	0.0525	0.0039	15	22.855	24.996
DCC parameter	θ_1	0.1009	0.0027	20	**35.233**	31.410
	θ_2	0.6775	0.0159			

The statistics column reports the Ljung–Box statistic on standardized residuals of duration, actual return changes and squared standardized residuals for different lags. The bold entries are the estimation coefficients that are not significantly different from zero and the Ljung–Box statistics that reject the non-correlation in the residuals.

determinist (seasonal factor) and random (error term) elements, we can further investigate the effect of the ex-ante liquidity risk embedded in the open LOB on the total risk. To this end, we define an impact coefficient of ex-ante liquidity risk:[19]

$$\Gamma_{int,\upsilon} = \frac{\widehat{LIVaR^c_{int,\upsilon}} - \widehat{IVaR^c_{int}}}{\widehat{LIVaR^c_{int,\upsilon}}}. \tag{15}$$

As mentioned above, $IVaR^c_{int,t}$ and $LIVaR^c_{int,\upsilon,t}$ are the VaRs for frictionless return changes and actual return changes of volume υ for the tth interval. As we simulate the data in the tick-by-tick framework, we can compute the $IVaR^c_{int,t}$ and $LIVaR^c_{int,\upsilon,t}$ for any desired interval. Accordingly, $\widehat{IVaR^c_{int}}$ and $\widehat{LIVaR^c_{int,\upsilon}}$ are the averages of $IVaR^c_{int,t}$ and $LIVaR^c_{int,\upsilon,t}$. As a result, $\Gamma_{int,\upsilon}$ assesses, on average, the impact of the ex-ante liquidity risk of volume υ on total risk for a given interval. Fig. 2 shows how the impact coefficients of ex-ante liquidity perform for intervals from 3 min to 10 min for the three stocks.

There are two interesting points to mention after observing the plots. First, the curve is globally increasing, that is, the impact coefficient of the ex-ante liquidity most often increases when the interval increases and finally converges to its long-run level. The relation of frictionless return changes and actual return changes can be explicitly expressed by $r_i^b = r_i^f + r_i^{LOB}$, where r_i^{LOB} is the volume-dependent LOB return change for the ith transaction. Econometrically, given that the sum of two ARMA structures is also an ARMA structure (Engel (1984)), the difference of the frictionless return changes and the actual return changes implicitly follows another ARMA structure. Accordingly, the relationship of $IVaR^c_{int,t}$ and $LIVaR^c_{int,\upsilon,t}$ can be generally written as:

$$LIVaR^c_{int,\upsilon,t} = IVaR^c_{int,t} + LOBIVaR^c_{int,\upsilon,t} + Dep^{F,LOB}_{int,\upsilon,t}. \tag{16}$$

$LOBIVaR^c_{int,\upsilon,t}$ measures the risk associated with the open LOB, and $Dep^{F,LOB}_{int,\upsilon,t}$ presents the dependence between the frictionless return changes and the actual return changes, which can stand for various dependence measures. However, in our specific modeling, $Dep^{F,LOB}_{int,\upsilon,t}$ is the covariance between r_i^f and r_i^{LOB}. Therefore, the numerator of Eq. (15) is the sum of $LOBIVaR^c_{int,\upsilon,t}$ and $Dep^{F,LOB}_{int,\upsilon,t}$. The fact that the curve is globally increasing in time is due to the higher autocorrelation in LOB return changes over time, which are the changes of magnitude in LOB caused by a given ex-ante volume.

The convergence means that, for the long run, the sum of $LOBIVaR^c_{int,\upsilon,t}$ and $Dep^{F,LOB}_{int,\upsilon,t}$ is proportional to $LIVaR^c_{int,\upsilon,t}$. Recall that in a general GARCH framework, the forward multi-step volatility converges to its unconditional level. In the present study, once the intervals include sufficient ticks for which the volatilities of both LOB return changes and frictionless return changes reach their unconditional levels, the volatilities of the sum of both return changes increase at the same speed. The impact coefficient of the ex-ante liquidity therefore converges to its asymptotic level.

[19] The risk measures in Eq. (15) are computed for confidence level 95%; in practice, other confidence levels can also be used.

Table 3
Backtesting on simulated deseasonalized data.

Nb of Interval	Interval (units)	Time interval (in Min)	Kupiec test				Christoffersen test				Unconditional coverage				I.I.D			
			5%	2.50%	1%	0.50%	5%	2.50%	1%	0.50%	5%	2.50%	1%	0.50%	5%	2.50%	1%	0.50%
Panel A: SAP out-of-sample backtesting on deseasonalized actual return change (v = 4000)																		
585	40	4.36	**0.001**	**0.010**	0.717	0.191	0.407	0.724	0.769	0.953	**0.019**	**0.008**	**0.000**	0.241	0.364	0.748	0.133	0.122
468	50	5.45	0.154	0.405	0.160	0.321	0.272	0.575	0.896	0.948	**0.006**	**0.006**	**0.018**	0.099	0.292	0.094	0.205	0.928
390	60	6.54	0.907	0.090	0.286	0.971	0.174	0.747	0.919	0.919	0.188	0.059	0.173	0.776	0.998	0.069	0.050	0.449
292	80	8.73	0.313	0.796	0.267	0.672	0.376	0.530	0.709	0.868	0.101	0.153	**0.024**	0.576	0.097	**0.014**	**0.007**	**0.010**
234	100	10.90	0.078	0.062	0.320	0.872	0.709	0.852	0.926	0.926	0.202	0.203	0.216	0.780	0.116	0.074	0.387	0.384
195	120	13.08	0.342	0.954	0.451	0.980	0.503	0.646	0.919	0.919	0.611	0.911	0.974	0.168	0.191	0.439	0.161	0.150
167	140	15.27	0.200	0.231	0.067	0.196	0.619	0.825	#	#	0.070	0.212	0.534	0.956	0.502	0.374	0.915	0.915
Panel B: RWE out-of-sample backtesting on deseasonalized actual return change (v = 4000)																		
535	40	4.77	**0.001**	**0.002**	0.095	0.239	0.477	0.832	0.902	0.951	**0.003**	**0.004**	**0.024**	0.226	0.951	0.876	0.690	0.667
428	50	5.96	0.134	0.589	0.891	0.923	0.313	0.557	0.783	0.891	0.299	0.212	0.322	0.383	0.661	0.427	0.514	0.689
357	60	7.14	0.217	0.292	0.362	0.874	0.341	0.679	0.881	0.881	0.066	0.207	0.051	0.107	0.171	0.442	0.204	0.083
267	80	9.55	0.106	0.258	0.239	0.761	0.510	0.762	0.931	0.931	0.084	0.130	0.790	0.713	0.664	0.528	0.535	0.689
214	100	11.92	0.109	0.877	0.577	0.126	0.591	0.661	0.811	0.811	**0.040**	0.098	0.592	0.855	0.970	**0.021**	**0.020**	**0.012**
178	120	14.33	0.145	0.460	0.522	0.909	0.590	0.748	0.915	0.915	**0.004**	**0.040**	0.235	0.351	0.819	0.625	0.317	0.632
153	140	16.67	0.626	0.299	0.646	0.797	0.538	0.817	0.908	0.908	0.722	0.088	0.253	0.864	0.059	0.884	**0.026**	0.742
Panel C: MRK out-of-sample backtesting on deseasonalized actual return change (v = 1800)																		
476	20	5.36	**0.006**	0.120	0.384	0.699	0.430	0.647	0.845	0.845	**0.001**	**0.032**	0.496	0.800	0.246	0.229	0.230	0.232
317	30	8.04	**0.026**	0.119	0.152	0.617	0.547	0.782	0.936	0.936	**0.008**	0.052	0.326	0.914	0.646	0.220	0.245	0.236
238	40	10.71	**0.021**	0.058	0.309	0.857	0.642	0.854	0.927	0.927	0.085	0.085	0.602	0.414	0.664	0.219	0.226	0.211
190	50	13.42	0.213	0.384	0.942	0.959	0.530	0.756	0.836	0.918	0.070	0.088	0.577	0.148	0.784	0.978	0.606	0.501
158	60	16.14	0.470	0.613	0.747	0.820	0.490	0.732	0.820	0.910	0.167	0.412	0.888	0.697	0.249	0.240	0.220	0.256
119	80	21.43	0.055	0.179	0.122	0.275	0.793	0.896	#	#	0.111	0.690	0.928	0.340	0.216	0.215	0.215	0.216
95	100	26.84	0.378	0.800	0.959	0.506	0.656	0.768	0.883	0.883	0.336	0.886	0.592	0.168	0.252	0.215	0.242	0.237

The table contains the *p*-values for Kupiec, Christoffersen, unconditional coverage, and I.I.D (Ziggel et al., 2014) tests for the stocks SAP, RWE and MRK. Interval is the interval length used for computing the LIVaR. Nb of intervals is the number of intervals for out-of-sample analysis and Time interval in minutes is the corresponding calendar time. Bold entries indicate the rejections of the model at 95% confidence level. When the number of hits is less than two, the *p*-values are denoted by #.

Table 4
Backtesting on simulated re-seasonalized data.

Interval (in mins)	Nb of interval	Kupiec test				Christoffersen test				Unconditional coverage				I.I.D			
		5%	2.50%	1%	0.50%	5%	2.50%	1%	0.50%	5%	2.50%	1%	0.50%	5%	2.50%	1%	0.50%
Panel A: SAP out-of-sample backtesting on re-seasonalized actual return change (v = 4000)																	
5	485	0.445	0.420	0.091	**0.017**	0.612	0.444	0.130	0.675	0.790	0.978	0.436	0.148	0.851	0.324	0.386	0.650
6	405	0.132	0.483	0.256	0.986	0.334	0.570	0.888	0.888	0.060	0.089	0.236	0.694	0.328	0.564	0.709	0.692
7	345	0.072	0.160	0.803	0.838	0.053	0.332	0.818	0.878	0.316	0.686	0.654	0.673	0.961	**0.006**	0.404	**0.038**
8	300	0.588	0.566	1.000	0.663	0.297	0.651	0.841	#	0.721	0.643	0.408	0.983	0.667	0.237	0.086	**0.016**
9	270	0.670	0.923	0.209	0.220	0.500	0.132	0.697	0.832	0.723	0.780	0.764	0.459	0.562	0.124	0.286	0.689
10	245	0.066	0.726	0.362	0.520	0.081	0.552	0.752	0.898	0.713	0.896	0.925	0.726	0.370	0.416	0.693	**0.020**
Panel B: RWE out-of-sample backtesting on re-seasonalized actual return change (v = 4000)																	
5	485	0.173	0.341	0.364	0.778	0.266	0.604	0.897	0.927	0.510	0.649	0.922	0.889	0.996	0.682	0.085	0.587
6	405	0.132	0.071	0.583	0.986	0.352	0.777	0.888	0.921	0.358	0.604	0.812	0.325	0.723	0.791	**0.008**	**0.005**
7	345	0.570	0.563	0.772	0.379	0.259	0.618	0.791	0.851	0.536	0.928	0.276	0.455	0.742	0.072	0.170	0.858
8	300	0.070	0.156	0.537	0.697	0.651	0.776	0.908	0.908	**0.002**	0.290	0.400	0.651	0.694	0.677	0.257	0.269
9	270	0.307	0.247	0.857	0.601	0.430	0.795	0.863	0.931	0.273	0.788	0.673	0.386	0.804	0.456	**0.001**	**0.001**
10	245	**0.043**	0.156	0.733	0.175	0.647	0.856	0.856	0.856	0.084	0.357	0.485	0.197	0.639	0.533	0.068	0.069
Panel C: MRK out-of-sample backtesting on re-seasonalized actual return return (v = 1800)																	
5	485	0.187	0.201	0.140	0.298	0.344	0.628	0.897	0.949	0.090	0.102	0.086	0.270	0.892	0.831	0.101	0.101
6	405	**0.010**	0.071	0.980	0.220	0.476	0.723	0.777	0.777	0.172	**0.046**	0.179	0.780	0.111	0.590	0.444	0.102
7	345	0.273	0.175	0.394	0.548	0.312	0.701	0.878	0.939	0.431	0.126	0.460	0.836	0.882	0.457	0.204	0.102
8	300	0.267	0.566	0.537	0.083	0.359	0.620	0.870	#	0.154	0.335	0.953	0.998	0.624	0.174	0.258	0.114
9	270	0.098	0.247	0.654	0.752	0.513	0.728	0.863	0.931	**0.013**	0.077	0.504	0.627	0.387	0.512	0.966	0.968
10	245	**0.016**	0.050	0.765	0.520	0.647	0.856	0.856	0.856	**0.002**	0.110	0.366	0.621	0.165	0.577	0.109	0.108

The table contains the *p*-values for Kupiec and Christoffersen, unconditional coverage, and I.I.D (Ziggel et al., 2014) tests. Intervals are regularly time–spaced from 5 min to 10 min. Bold entries indicate the rejections of the model at 95% confidence level. When the number of hits is less than two, the *p*-values are denoted by #.

Second, it is interesting to observe that the impact coefficients of ex-ante liquidity of the RWE stock are negative for a volume of 1000 shares and become positive when volumes are 2000, 3000 and 4000 shares. A negative impact coefficient of ex-ante liquidity indicates that volatility for the actual return changes is less than that of the frictionless return changes. In other words, the ex-ante liquidity risk embedded in LOB offsets the market risk. This again results from the fact that off-best levels of LOB are more stable than the first level. Based on Eq. (16), when the volume is small, the negative correlation between frictionless return change and LOB return change plays a more important role in determining the sign of the impact coefficients of ex-ante liquidity. However, for a higher ex-ante volume, the risk of LOB return change also increases but at a faster rate than its interaction with frictionless return change. Consequently, the impact coefficients of ex-ante liquidity become positive.

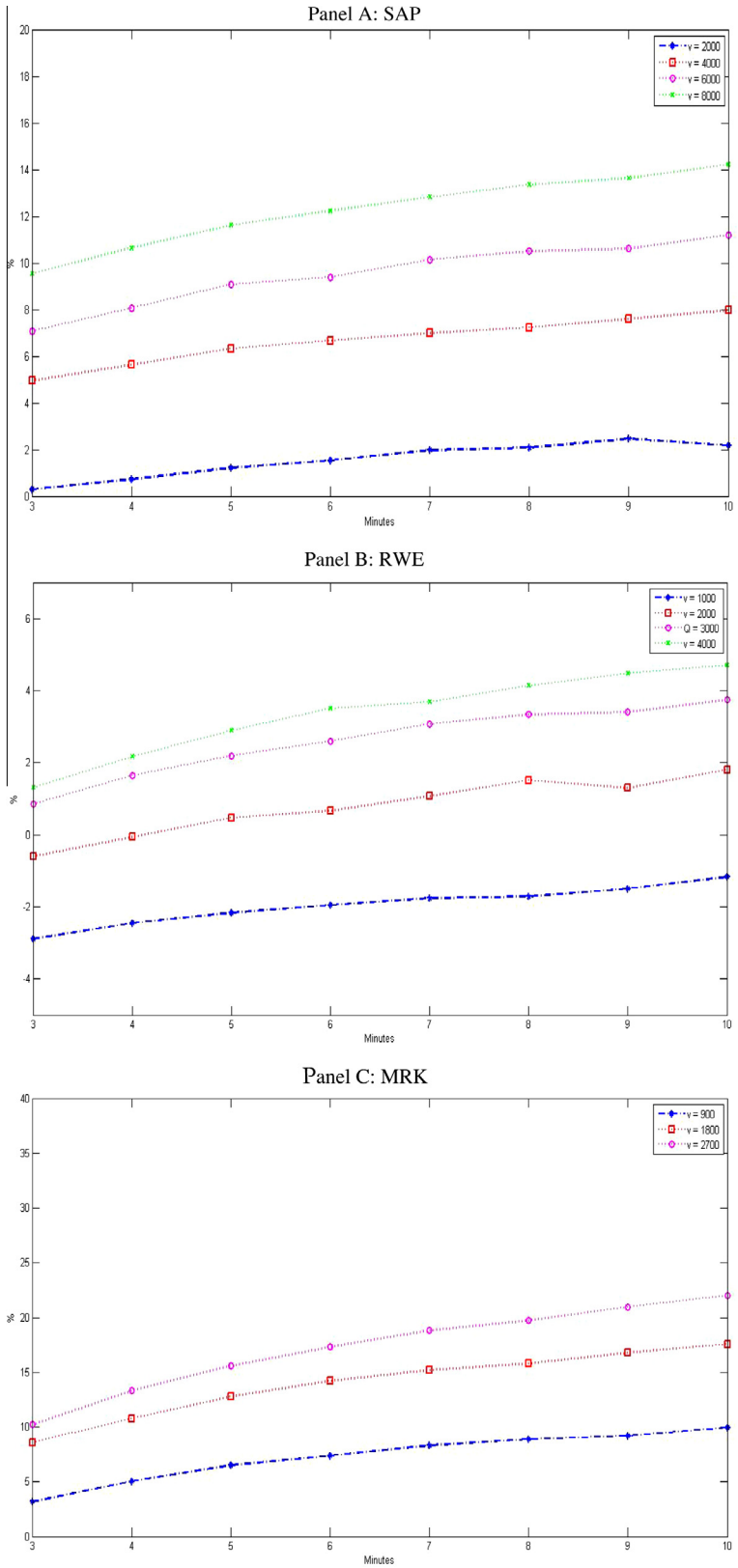

Fig. 2. Impact coefficients of ex-ante liquidity for different time intervals. Panels A, B and C illustrate how the impact coefficients of ex-ante liquidity evolve for intervals from 3 min to 10 min for stocks SAP, RWE and MRK. The selected volumes for the actual return changes are 2000, 4000, 6000 and 8000 shares for SAP, 1000, 2000, 3,000 and 4000 shares for RWE, and 900, 1800 and 2700 shares for MRK.

7.2. High-frequency ex-ante liquidity premium

Based on the tick-by-tick simulation, we can also compute the high-frequency IVaR and LIVaR for frictionless return and actual return. Using IVaR and LIVaR of the same stock, we can further define a Relative Liquidity Risk Premium as follows:

$$\Lambda_{int,v,t} = \frac{LIVaR_{int,v,t} - IVaR_{int,t}}{LIVaR_{int,v,t}}. \quad (17)$$

Similar to the liquidity ratio proposed in Giot and Grammig (2006), $IVaR_{int,t}$ and $LIVaR_{int,v,t}$ are the VaR measures for frictionless return and actual return at the end of the t-th interval and int is the predetermined interval such as 5-min and 10-min. Unlike the frictionless return changes and actual return changes, our defined actual return and frictionless return do not have the time-additivity property. Even though the VaR based on frictionless return changes and actual return changes can be used directly in practice, in some situations practitioners might want to predict their potential loss on frictionless return or actual return instead of frictionless and actual return changes for a precise calendar time point.

To illustrate how our model can be used to provide the ex-ante risk measure for frictionless return and actual return, we first compute the return changes for frictionless returns and actual returns, then calculate the instantaneous frictionless return and actual return at the beginning of the given interval using Eqs. (3) and (4). Once we know the frictionless return and actual return at the beginning of a given interval, we can obtain the frictionless return and actual return for the end of the interval. Fig. 3 illustrates how the frictionless return and actual return at the end of an interval are computed. Fig. 4 tracks the evolution of IVaR and LIVaR associated with a large liquidation volume for SAP, RWE and MRK during one out-of-sample day, July 12, 2010. For the three stocks, the IVaR and LIVaR both present an inverted U shape during the trading day. However, for the more liquid stock SAP, the IVaR and LIVaR are less volatile than those of the less liquid stocks RWE and MRK. It also seems that the total risk is smaller during the middle of the day. Nonetheless, the smaller VaR in absolute terms does not mean we should necessarily trade at that moment. The IVaR and LIVaR only provide the estimates of potential loss for a given probability at a precise point in time.

In addition, the difference between the curves on each graph, which measures the risk associated with ex-ante liquidity, varies with time. This occurs because LOB interacts with trades and changes during the trading days. A smaller (bigger) difference indicates a deeper (shallower) LOB. More specifically, for the least liquid stock, MRK, the ex-ante liquidity risk is more pronounced even for a relatively smaller quantity of 1800 shares. Regarding the more liquid stocks such as SAP and RWE, the ex-ante liquidity risk premiums are much smaller even for the relatively larger quantities of 4000 shares. This again suggests that the ex-ante liquidity risk heightens when the liquidation quantity is large and the stock is less liquid.

Table 5 presents the average relative ex-ante liquidity risk premium given various order sizes at different confidence levels for SAP, RWE and MRK. The results are based on our one-week simulations. For each stock, we consider order sizes ranging from the mean to the 99th quantile of historical transaction volume. As shown in Table 5, the proportion of liquidity risk increases with volume for the three stocks, as expected. At the 95% confidence level, for the average transaction volumes the liquidity risk accounts for only 3.46%, 2.88% and 1.03% of total risk for SAP, RWE and MRK, respectively, meaning that the LOB seems efficient for providing liquidity for relatively small transaction volumes. However, for large transaction volumes such as the 99th quantile, liquidity risk can account for up to 32%, 25.26% and 31.88% of total risk at 95% confidence level.

7.3. Comparison of LIVaR and other intraday VaRs

Our proposed IVaR and LIVaR, which are validated by backtesting, allow us to further analyze ex-ante liquidity and compare the two risk measures with other high-frequency risk measures found in the literature.

The standard IVaR proposed by Dionne et al. (2009) is based on a transaction price that is similar to the closing price in daily VaR computation. However, the resulting IVaR serves as a measure of potential loss of 'paper value' for a frozen portfolio and omits the ex-ante liquidity dimension. To some extent, the IVaR accounts for an ex-post liquidity dimension; more specifically, it measures the liquidity already consumed by the market. However, active traders are more concerned with ex-ante liquidity because it is related to their liquidation value. For any trader, the risk related to liquidity is always present and the omission of this liquidity dimension can cause a serious distortion from the observed transaction price, especially when the liquidation volume is large.

Another major difference is that before obtaining LIVaR, we should compute $LIVaR^c$ for actual return changes, which gives the potential loss in terms of waiting costs over a predetermined interval. Accordingly, the resulting LIVaR provides a risk measure for actual return at a given point in time, while the standard IVaR is based on tick-by-tick log-returns, which have a time-additive

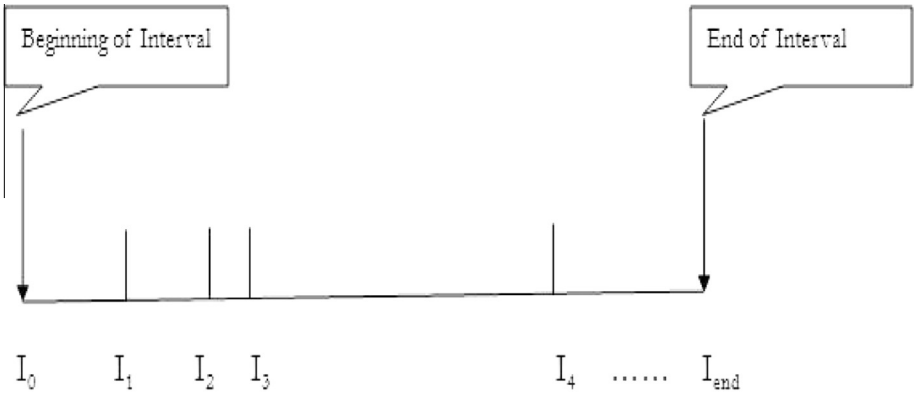

Fig. 3. Computation of the frictionless return and the actual return for the end of an interval. Illustrates the computation of the frictionless return and the actual return for the end of an interval. I indicates the transaction. At the beginning of the interval, we compute the frictionless return and actual return using real market data. Each I corresponds to a frictionless (actual) change that comes from the simulations. Consequently, the frictionless return (actual return) at the end of the interval is the sum of the initial frictionless return (actual return) and all the corresponding changes in the interval.

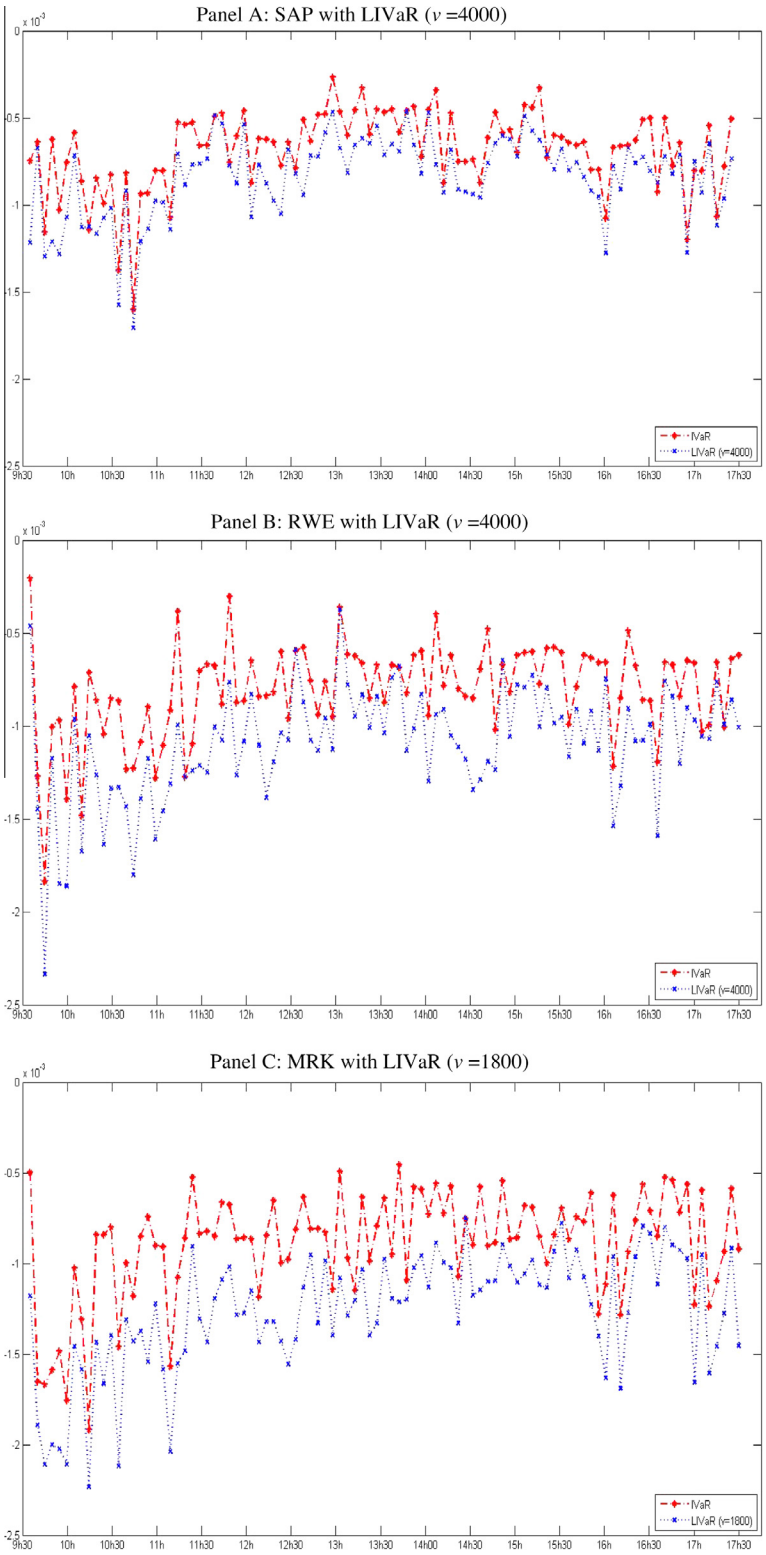

Fig. 4. IVaR and LIVaR of 5-min for July 12, 2010. Panels A, B and C present the VaRs for frictionless returns and actual returns at the end of each 5-min interval on July 12, 2010, for the three stocks of SAP, RWE and MRK, respectively. The selected volumes for the actual returns are 4000 shares for SAP, 4000 shares for RWE and 1800 shares for MRK.

property. It thus directly gives a risk measure in terms of price for a given interval.

The high-frequency VaR proposed by Giot and Grammig (2006) is constructed on mid-quote price and ex-ante liquidation price over an interval of 10 or 30 min. As mentioned in Section 3, because the use of mid-quote might underestimate the risk faced by active traders, we take best bid price as the frictionless price when liquidating a position. Fig. 5 illustrates the difference in constructing the frictionless returns and actual returns.

Consequently, for active day-traders, our LIVaR can be considered an upper bound of risk measure that provides the maximum p-th quantile in absolute value when liquidating a given volume v.

Table 5
The relative liquidity risk premium.

Relative ex-ante liquidity risk premium at the end of 5-min interval					
Confidence level	Volume (shares)/PDHTV				
	550 Mean	1500 >90%	2000 >95%	4000 >97.5%	8000 >99%
Panel A: SAP					
10%	4.03%	10.36%	12.86%	22.20%	34.17%
5%	3.46%	9.32%	11.58%	20.55%	32.00%
1%	2.72%	8.22%	10.26%	18.40%	29.24%
Panel B: RWE					
Confidence level	Volume (shares)/PDHTV				
	350 Mean	1000 >90%	1500 >95%	2000 >97.5%	4000 >99%
10%	3.62%	9.78%	14.57%	17.82%	27.80%
5%	2.88%	8.39%	12.87%	15.92%	25.26%
1%	2.09%	6.54%	10.55%	13.45%	21.76%
Panel C: MRK					
Confidence level	Volume (shares)/PDHTV				
	200 Mean	500 >90%	900 >95%	1800 >97.5%	2700 >99%
10%	1.96%	9.83%	16.66%	27.07%	33.40%
5%	1.03%	8.96%	15.81%	25.79%	31.88%
1%	0.39%	8.67%	15.12%	24.65%	30.18%

The panels present the proportion of liquidity risk on total risk given different order sizes at 90%, 95% and 99% confidence level for SAP, RWE and MRK. The order size for each stock ranges from the average (first column) to the 99th quantile of transaction volume (last column). PDHTV: Percentile in the Distribution of Historical Trade Volume.

Further, we found that durations impact volatilities of both frictionless and actual returns (with a higher impact on actual returns than on frictionless returns), and therefore should not be ignored.

8. Robustness analysis

In the following subsections, we conduct further analysis to investigate to what extent our results based on two weeks of high-frequency data can be generalized.

8.1. Another sample period

To address the concern that our findings are sample dependent, we apply the same methodology to the three stocks for a different two-week period (June 6–June 17, 2011). The results are presented in the web-appendix. The descriptive statistics in Table A1 as well as the daily and intradaily plots from Figs. A2–A7 indicate differences in terms of price, trading volume and price impact for a given quantity between the two sample periods for each of the three stocks. For example, MRK appears more liquid in the second sample period when the price impact for a given quantity is less pronounced. However, the trading volume, on average, decreases during the second sample period. We also observe that the price patterns, which are accompanied by different volatility patterns, also differ for these two sample periods.

The model structure used remains the same, that is, the LogACD-VARMA-MGARCH model. However, the seasonality and the number of lags for the three parts of the model naturally change depending on the characteristics of the trading data and LOB structure. Backtesting results indicate that our proposed procedure delivers reliable high-frequency risk measures. As expected, due to different characteristics in trading and LOB structure, the results regarding the average relative ex-ante liquidity risk premium are somewhat different. For example, the LOB of SAP in June 2011 is less deep than in July 2010. As illustrated in Fig. A5, the price impact for a given quantity is larger for June 2011. As a result, the average relative ex-ante liquidity risk premium slightly increases. For MRK, we have the opposite situation: the depth of the LOB increases in 2011 compared to 2010; thus, not surprisingly, the average relative ex-ante liquidity risk premium decreases.

8.2. Simulations

Next, we design a simulation experiment to quantify the impact of volatility changes on the ex-ante liquidity risk premium. Using simulations allows us to investigate how these changes influence the liquidity risk premium. To this end, we define two possible and realistic scenarios based on the characteristics of an open

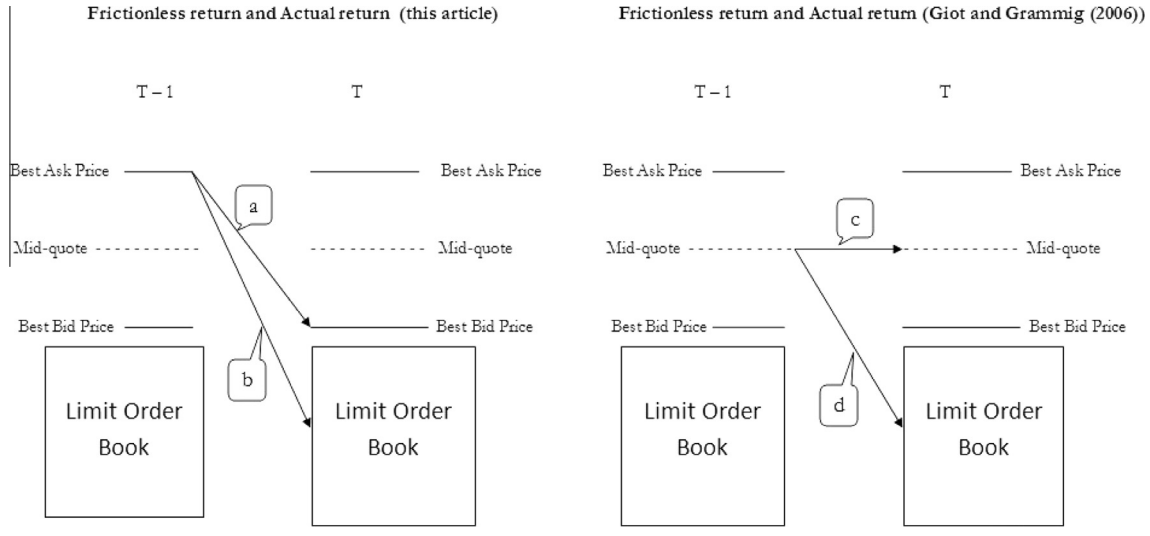

Fig. 5. Frictionless returns and actual returns. This figure presents the difference between our frictionless (actual) return and the frictionless (actual) return proposed by Giot and Grammig (2006). Arrow *a* presents the starting price and end price in constructing our frictionless return, while arrow *b* shows the starting price and end price for the actual return given a liquidation quantity *v*. Both frictionless returns and actual returns take the previous best ask price as starting price. Arrows *c* and *d* give the starting price and end price for computing the frictionless return and the actual return (for quantity *v*) proposed by Giot and Grammig (2006). Their frictionless return takes the previous mid-quote as the starting price and the following mid-quote as the end price. Their actual return takes the previous mid-quote as the starting price and the actual price as the end price.

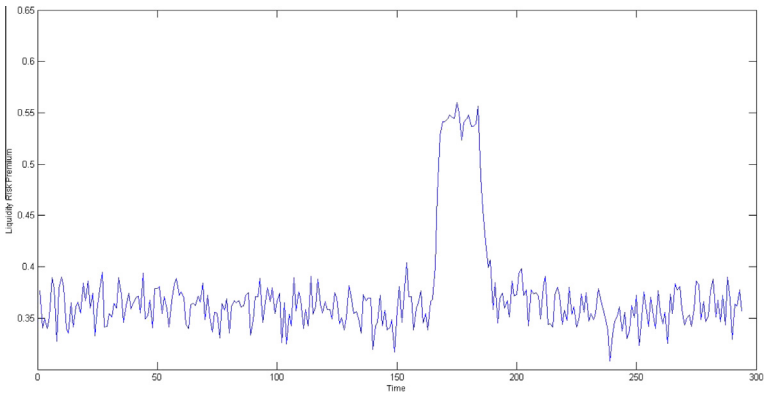

Fig. 6. The effect of short-lived extreme events on liquidity risk premium. Presents the evolution of liquidity risk premium with short-lived extreme events in Best Bid and LOB. The negative shocks for actual return changes and frictionless return changes represent the 5% and 2% quantiles of corresponding empirical distribution, respectively. The time interval is 30 units and the confidence level is 2.5%.

LOB trading system. In the first scenario, we suppose that the volatility of actual returns reaches a higher level for the whole sample period while the volatility of frictionless return remains the same. Recall that the frictionless return is a component in actual return; therefore, the first scenario implies that the LOB (depth and price beyond the first level) becomes more volatile than the best price during the whole sample period. By simulating different sets of volatilities, we are able to follow and compare the average impact of LOB volatility on liquidity risk premium. In the second scenario, we are interested in the impact of (adverse) short-lived extreme events on the liquidity risk premium. Compared to the first scenario in which we focus on the average impact for a given set of volatilities, in the second scenario, we pay attention to the time series of liquidity risk premium, especially during the occurrence of the short-lived extreme events.

The procedure for the first scenario is as follows: first, we choose the estimated parameters for MRK for a liquidation volume equal to 2700 as the initial parameters. Second, we modify the volatility of actual return changes but keep the volatility of frictionless return changes unchanged and simulate 5000 scenarios for this magnitude of volatility. In our exercise, we choose 14 different volatility multipliers ranging from 1.05 to 5 times the initial volatility. Third, we compute the liquidity risk premium based on the simulated data. Fig. A8 in the web-appendix illustrates the pattern of liquidity risk premium as a function of volatility. Ceteris paribus, as the volatility of LOB becomes higher, traders will be exposed to a higher liquidity risk for a given volume. Our initial liquidity risk premium is around 30%.[20] However, with a 5 times higher volatility of actual return changes, this premium becomes around 65%.

For the second simulation scenario, we keep the same initial parameters as for the first scenario. In order to generate the shocks of short-lived extreme events, we predetermine a time interval for which we assign negative shocks to actual return and frictionless return.[21] Beyond this time interval, the shocks will be generated randomly as before. Fig. 6 shows how the liquidity risk premium evolves during the whole sample period when a short-lived extreme event occurs. Without the short-lived extreme events, the liquidity risk premium is around 35%,[22] whereas during the extreme events, the liquidity risk premium goes up to 55%.[23]

In conclusion, the two simulation exercises seem to indicate that the liquidity risk premium increases less rapidly than the total risk for actual return.

9. Conclusion

In this paper, we introduce the ex-ante liquidity dimension in an intraday VaR measure using tick-by-tick data. To take the ex-ante liquidity into account, we first reconstruct the LOB for three blue-chip stocks actively traded in Deutsche Börse (SAP, RWE and MRK) and define the tick-by-tick actual return, that is, the log ratio of ex-ante liquidation price computed from a predetermined volume over the previous best ask price. Correspondingly, the proposed $IVaR^c$ and $LIVaR^c$ are based on the frictionless return changes and actual return changes and relate to the ex-ante loss in terms of frictionless return and actual return, respectively. In other words, both risk measures can be considered as the waiting costs associated with market risk and liquidity risk.

To model the dynamic of returns, we use a LogACD-VARMA-MGARCH structure that allows for both the irregularly spaced durations between two consecutive transactions and stylized facts in changes of return. In this setup, the time dimension is supposed to be strongly exogenous. Once the model is estimated, Monte Carlo simulations are used to make multiple-step forecasts. More specifically, the Log-ACD process first generates the tick-by-tick duration while the VARMA-MGARCH simulates the corresponding conditional tick-by-tick frictionless return changes and actual return changes. The model performance is assessed by using the tests of Kupiec (1995), Christoffersen (1998) and the new backtests of Ziggel et al. (2014) on both simulated deseasonalized and re-seasonalized data. All tests indicate that our model can capture well the dynamics of frictionless returns and actual returns over various time intervals for confidence levels of 95%, 97.5%, 99% and 99.5%.

Our LIVaR provides a reliable measure of total risk for short horizons. In addition, the simulated data from our model can be easily converted to data in calendar time. In our sample, we find that the liquidity risk can account for up to 35% of total risk depending on order size. Similar results are obtained when using

[20] The liquidity risk premium is computed from LIVaR and IVaR with confidence level of 5% and time interval of 10 units.

[21] Our extreme event analysis is similar to Alexander and Sheedy (2008). The difference is that our simulation is done tick-by-tick, thus we cannot fix a precise time for the negative shocks. Our pre-determined time interval, which is arbitrary, could vary from several minutes to several hours. The negative shocks are assigned in the following way: we first draw a random number from a uniform distribution (0,1). When the number is higher than a given threshold, negative shocks are assigned; otherwise, the shocks are generated from our assumed distribution.

[22] The liquidity risk premium is computed from LIVaR and IVaR with confidence level of 2.5% and time interval of 30 units.

[23] The negative shocks for actual return changes and frictionless return changes represent the 5% and 2% quantiles of corresponding empirical distribution, respectively.

an alternative sample period. In a simulated environment, we find that the liquidity risk premium increases when the LOB becomes more volatile or during the period of an (adverse) short-lived extreme event.

Regarding practical applications, potential users of our measure could be high-frequency traders that need to specify and update their trading strategies within a trading day, or market regulators who aim to track the evolution of market liquidity, along with brokers and clearinghouses that need to update their clients' intraday margins.

Future research could take several directions. Our study is focused on a single stock's ex-ante liquidity risk. A possible alternative is to investigate how IVaR and LIVaR evolve in the case of a portfolio. In particular, the lack of synchronization of the durations between two consecutive transactions for each stock is a challenge. Another direction is to test the role of ex-ante liquidity in different regimes. Our study focuses on the liquidity risk premium in a relatively stable period. It could also be interesting to investigate how the liquidity risk behaves when there are randomly two possible regimes. This study will require a more complicated econometric model to take different regimes into account.

Appendix A. Supplementary data

Supplementary data associated with this article can be found, in the online version, at http://dx.doi.org/10.1016/j.jbankfin.2015.06.005.

References

Aït-Sahalia, Y., Saglam, M., 2014. High Frequency Traders: Taking Advantage of Speed. Working Paper, Princeton University, 50 pages.

Alexander, C., Sheedy, E., 2008. Developing a stress testing framework based on market risk models. Journal of Banking & Finance 32, 2220–2236.

Anatolyev, S., Shakin, D., 2007. Trade intensity in the russian stock market: dynamics, distribution and determinants. Applied Financial Economics 17, 87–104.

Andersen, T.G., Bollerslev, T., 1997. Intraday periodicity and volatility persistence in financial markets. Journal of Empirical Finance 4, 115–158.

Angelidis, T., Benos, A., 2006. Liquidity adjusted value-at-risk based on the components of the bid-ask spread. Applied Financial Economics 16, 835.

Bacidore, J., Ross, K., Sofianos, G., 2003. Quantifying market order execution quality at the New York stock exchange. Journal of Financial Markets 6, 281–307.

Bangia, A., Diebold, F.X., Schuermann, T., Stroughair, J.D., 1999. Modeling Liquidity Risk With Implications for Traditional Market Risk Measurement and Management. The Wharton Financial Institutions Center WP 90-06.

Battalio, R., Hatch, B., Jennings, R., 2003. All else equal?: a multidimensional analysis of retail, market order execution quality. Journal of Financial Markets 6, 143–162.

Bauwens, L., Giot, P., 2000. The logarithmic ACD model: an application to the bid-ask quote process of three NYSE stocks. Annals of Economics and Statistics/Annales d'Économie et de Statistique 60, 117–149.

Beltran-Lopez, H., Giot, P., Grammig, J., 2009. Commonalities in the order book. Financial Markets and Portfolio Management 23, 209–242.

Bilodeau, Y., 2013. Xetraparser [computer software]. HEC Montréal.

Black, F., 1971. Toward a fully automated stock exchange. Financial Analysts Journal 27, 28–44.

Bloomfield, R., O'Hara, M., Saar, G., 2005. The "make or take" decision in an electronic market: evidence on the evolution of liquidity. Journal of Financial Economics 75, 165–199.

Brogaard, J., Hendershott, T., Riordan, R., 2014. High-frequency trading and price discovery. Review of Financial Studies 27, 2267–2306.

Chaboud, A., Chiquoine, B., Hjalmarsson, E., Vega, C., 2014. Rise of the machines: algorithmic trading in the foreign exchange market. Journal of Finance 69, 2045–2084.

Christoffersen, P.F., 1998. Evaluating interval forecasts. International Economic Review 39, 841–862.

Christoffersen, P.F., 2003. Elements of Financial Risk Management. Academic Press, San Diego, 214.

Coppejans, M., Domowitz, I., Madhavan, A., 2004. Resiliency in an Automated Auction. Working Paper.

Demsetz, H., 1968. The cost of transacting. Quarterly Journal of Economics 82, 33–53.

Dionne, G., Duchesne, P., Pacurar, M., 2009. Intraday value at risk (IVaR) using tick-by-tick data with application to the toronto stock exchange. Journal of Empirical Finance 16, 777–792.

Domowitz, I., Hansch, O., Wang, X., 2005. Liquidity commonality and return co-movement. Journal of Financial Markets 8, 351–376.

Dufour, A., Engle, R.F., 2000. Time and the price impact of a trade. Journal of Finance 55, 2467–2498.

Dufour, J.-M., Pelletier, D., 2011. Practical Methods for Modelling Weak VARMA Processes: Identification, Estimation and Specification with a Macroeconomic Application. Working Paper.

Engel, E.M.R.A., 1984. A unified approach to the study of sums, products, time-aggregation and other functions of ARMA processes. Journal of Time Series Analysis 5, 159–171.

Engle, R.F., 2000. The econometrics of ultra-high-frequency data. Econometrica 68, 1–22.

Engle, R., 2002. Dynamic conditional correlation: a simple class of multivariate generalized autoregressive conditional heteroskedasticity models. Journal of Business & Economic Statistics 20, 339–350.

Engle, R.F., Ng, V.K., 1993. Measuring and testing the impact of news on volatility. Journal of Finance 48, 1749–1778.

Engle, R.F., Russell, J.R., 1998. Autoregressive conditional duration: a new model for irregularly spaced transaction data. Econometrica 66, 1127–1162.

Engle, R.F., Sheppard, K., 2001. Theoretical and Empirical properties of Dynamic Conditional Correlation Multivariate GARCH. NBER Working Papers.

Foucault, T., Kadan, O., Kandel, E., 2005. Limit order book as a market for liquidity. Review of Financial Studies 18, 1171–1217.

Ghysels, E., Jasiak, J., 1998. GARCH for irregularly spaced financial data: the ACD-GARCH model. Studies in Nonlinear Dynamics & Econometrics 2, 133–149.

Giot, P., Grammig, J., 2006. How large is liquidity risk in an automated auction market? Empirical Economics 30, 867–887.

Glosten, L.R., Harris, L.E., 1988. Estimating the components of the bid/ask spread. Journal of Financial Economics 21, 123–142.

Gouriéroux, C., Jasiak, J., 2010. Local likelihood density estimation and value-at-risk. Journal of Probability and Statistics, 26.

Goyenko, R.Y., Holden, C.W., Trzcinka, C.A., 2009. Do liquidity measures measure liquidity? Journal of Financial Economics 92, 153–181.

Grammig, J., Maurer, K.-O., 2000. Non-monotonic hazard functions and the autoregressive conditional duration model. Econometrics Journal 3, 16–38.

Handa, P., Schwartz, R.A., 1996. Limit order trading. Journal of Finance 51, 1835–1861.

Hautsch, N., 2004. Modelling irregularly spaced financial data: theory and practice of dynamic duration models. Lecture Notes in Economics and Mathematical Systems, vol. 539. Springer, Berlin, p. 292.

Hendershott, T., Jones, C.M., Menkveld, A.J., 2011. Does algorithmic trading improve liquidity? Journal of Finance 66, 1–33.

Irvine, P.J., Benston, G.J., Kandel, E., 2000. Liquidity beyond the inside spread: measuring and using information in the limit order book. SSRN eLibrary.

Kaniel, R., Liu, H., 2006. So what orders do informed traders use? Journal of Business 79, 1867–1913.

Kumar, P., Seppi, D.J., 1994. Limit and market orders with optimizing traders. SSRN eLibrary.

Kupiec, P., 1995. Techniques for verifying the accuracy of risk measurement models. Journal of Derivatives 2, 73–84.

Kyle, A.S., 1985. Continuous auctions and insider trading. Econometrica 53, 1315–1335.

Pacurar, M., 2008. Autoregressive conditional duration models in finance. a survey of the theoretical and empirical literature. Journal of Economic Surveys 22, 711–751.

Rosu, I., 2009. A dynamic model of the limit order book. Review of Financial Studies 22, 4601–4641.

Weiß, G.N.F., Supper, H., 2013. Forecasting liquidity-adjusted intraday value-at-risk with vine copulas. Journal of Banking & Finance 37, 3334–3350.

Zhang, M.Y., Russell, J.R., Tsay, R.S., 2001. A nonlinear autoregressive conditional duration model with applications to financial transaction data. Journal of Econometrics 104, 179–207.

Ziggel, D., Berens, T., Weiß, G.N.F., Wied, D., 2014. A new set of improved value-at-risk backtests. Journal of Banking & Finance 48, 29–41.